

***Ab initio* study of boron, nitrogen, and boron–nitrogen clusters. I. Isomers and thermochemistry of B₃, B₂N, BN₂, and N₃**

J. M. L. Martin

Limburgs Universitair Centrum, Department SBM, Universitaire Campus, B-3610 Diepenbeek, Belgium and University of Antwerp (UIA), Institute for Materials Science, Department of Chemistry, Universiteitsplein 1, B-2610 Wilrijk, Belgium

J. P. François

Limburgs Universitair Centrum, Department SBM, Universitaire Campus, B-3610 Diepenbeek, Belgium

R. Gijbels

University of Antwerp (UIA), Institute for Materials Science, Department of Chemistry, Universiteitsplein 1, B-2610 Wilrijk, Belgium

(Received 14 December 1988; accepted 23 January 1989)

For a number of different structures and states of B₃, B₂N, BN₂, and N₃, optimum geometries and harmonic spectra were obtained at the HF/6-31G* level. The relative stability of the isomers was determined using full fourth-order Møller–Plesset theory, both with and without spin projection, as well as coupled cluster methods. Estimates for the dissociation energies are based on scaled CCD + ST(CCD) binding energies. Koopmans' vertical ionization potentials and Mulliken charge distributions, both at the UHF/6-31G* level, are quoted for the most stable isomers. B₃ is found to be an equilateral triangle in its ²A₁' ground state. B₂N has a symmetric linear arrangement in its ²Σ_u⁺ ground state with an extremely low bending frequency (73 cm⁻¹), and an unusually low vertical ionization potential (6.75 eV). Its asymmetric stretching (2021 cm⁻¹) is found to be extremely intense (8782 km mol⁻¹). BN₂ has four rather closely spaced states, of which an isosceles triangle is the absolute minimum (²A₁ state). However, at high temperatures, an asymmetric linear arrangement (²Π state) is found to have equal importance, whereas a ⁴Σ⁻ state plays a role there too. The same theoretical methods correctly predict for N₃ a symmetric linear arrangement in the ²Π_g ground state; the spectroscopic constants are found to be in reasonable agreement with experiment. Estimated dissociation energies (expected accuracy ± 4 kcal mol⁻¹) are: B₃ 197.9, B₂N 265.0, BN₂ 224.9, N₃ 210.1 kcal mol⁻¹. From a statistical thermodynamical analysis, B₃ is stable against dissociation to B₂ and B up to very high temperatures, B₂N is extraordinarily stable, whereas BN₂ and N₃ dissociate spontaneously to B + N₂ and N + N₂ at all temperatures. From these results, the presence of B₂N⁺ and B₃⁺, the high abundance of B₂N⁺, as well as the absence of BN₂⁺ and N₃⁺ in laser mass spectra of boron nitride is explained.

I. INTRODUCTION

Boron nitride (BN) is a chemically inert refractory material. Many applications have been found: for a review, the reader is referred to Ref. 1. Boron nitride forms several phases, analogous to those of carbon: hexagonal α-BN resembling graphite, the sphalerite-type β-BN, and the wurtzite-type γ-BN, resembling cubic and hexagonal diamond, respectively. Like their carbon counterparts, the latter two phases are metastable under normal temperature and pressure conditions. They can only be formed from α-BN under very high temperature and pressure.

BN can be obtained from several reactions, including diborane-ammonia, boron trifluoride-ammonia, and borane triethylamine-ammonia. Thin solid BN films can be obtained among others by the following methods¹: r.f. sputtering, "chemical vapor deposition" (CVD), "laser pulse vapor deposition" (LPVD), "ionized cluster beam deposition" (ICB).² It has proven extremely difficult to obtain β or γ BN as a thin solid film. BN films, prepared by r.f. sputtering from an α BN target under N₂ or N₂-Ar atmosphere, were shown to be α BN by IR and TEM investigations.^{3,4} BN

films containing the β and γ phases, along with α BN, were obtained by plasma deposition,^{5,6} and by deposition from boron vapor irradiated with a N₂⁺ ion beam.⁷

γ BN depositions on a substrate were obtained by LPVD with a γ BN target under nitrogen atmosphere.⁸ Experimental research is now conducted⁹ as to the relationship between the target state, the plasma composition, and the composition and phase distribution of the deposited product. Important components of the plasma are B_n, N_n, and B_mN_n clusters, as well as their positive and negative ions. It is seen, that the cluster composition of the plasma is of essential importance for the properties of the deposited BN material. The clusters form a "natural bridge," as it were, between individual BN molecules and the solid state. For that reason, the abundance distributions of the clusters are used for plasma diagnostics; additionally, the cluster properties are of importance for understanding the mechanism of formation and the evolution of the deposited product.

However, scarcely any experimental data are available as to the properties of these clusters, except for N₂, where a vast amount of theoretical¹⁰ as well as experimental¹¹ data can be found in literature. *Ab initio* molecular orbital calcula-

tions seem a helpful alternative at this stage: because of this, such a study was undertaken in our laboratory, starting with the neutral $B_m N_{3-m}$ ($m = 0, \dots, 3$) clusters discussed in this paper.

Besides the practical importance of these results, the properties of such clusters are also of theoretical interest. Carbon clusters have been well studied now.¹² Boron and nitrogen clusters are “neighbors” in the Periodic Table, while the mixed clusters and their ions are sometimes isoelectronic with the carbon species (but with lower symmetry). From a purely theoretical viewpoint, it would be interesting to compare the chemical bonding in these clusters with each other, especially with regards to the nature of the various stationary points.

For B_2 , reliable experimental¹¹ and theoretical¹³ data also exist. For BN, the experimental data¹¹ are already incomplete; MRD-CI calculations have been performed by Karna and Grein.¹⁴ A survey of the theoretical and experimental data regarding the higher clusters would be very brief: the only more or less systematic investigation was conducted by Novaro *et al.*¹⁵ for the N_3 surface, here considered in comparison with the P_3 surface. Their investigation was conducted using a simple split-valence basis set and Hartree–Fock theory, so it seems somewhat outdated. On the other hand, there have been numerous calculations¹⁶ on the electron affinity of the azide ion, in which the N_3 species also appears. However, no potential surface study was conducted in these studies. For N_3 , good experimental (spectroscopical) data have been given recently.¹⁷ No theoretical or experimental data at all are available for B_3 , B_2N , or BN_2 . The only exception is a very recent study of boron–nitrogen clusters by Seifert *et al.*,¹⁸ using a simplified LCAO-LDA (local density approximation) method¹⁹ which is questionable for obtaining quantitative and even qualitative results. It should also be remarked, that no geometry optimization was carried out by these authors: they assumed linear geometries with fixed bond distances for the three-membered clusters. No distinction was made between electronic states. Results for N_2 and B_2 are so blatantly imprecise (errors of about 100% on the binding energy) that any conclusions presented in that paper should be taken with some caution.

II. COMPUTATIONAL METHODS

All computations were carried out using the GAUSSIAN 86²⁰ program package, running on a MicroVAX 2000 workstation under VMS 4.7. Unrestricted Hartree–Fock theory²¹ has been used throughout.

First, a small topological study was made with the help of some MNDO²² calculations, for identifying some probable structures. Although very helpful in obtaining reasonable starting geometries, the results *per se* are often deceptive: for example, a false Jahn–Teller distortion was found for the cyclic B_3 doublet structure, in complete contradiction with the results at the *ab initio* level shown below.

From these results, geometry optimizations were carried out at the UHF/3-21G²³ level, using the built-in Berny optimization method by Schlegel.²⁴ Since the initial estimate²⁵ for the Hessian is inappropriate for cyclic and “outlandish” structures, the second derivative matrix has been

calculated analytically on the first step. Problems were less prone than at the MNDO level; however, compared with the 6-31G* final results, the 3-21G equilibrium geometries were far more problematic than their MNDO counterparts. On the N_3 surface, some of the 6-31G* stationary points even failed to converge at the 3-21G level.

From the 3-21G equilibrium geometry, an optimization using the standard 6-31G* basis²⁶ was carried out. The updated force constant matrix from the 3-21G calculation was used to start the optimization: the final wave function of the latter was projected to obtain a reliable initial guess. The convergence criteria were tightened, to reduce translational and rotational contamination in the subsequent force constant matrix calculation.

Subsequently, a harmonic frequency calculation was carried out using analytic second derivatives.²⁷ The most abundant isotopes, i.e., ¹¹B and ¹⁴N, are used throughout. The results, along with the symmetry assignment of the normal vibrations, are shown in Table III. The computed zero point energy is given in the last column of that table: for transition states, the imaginary frequency was disregarded. At very little extra expense, the IR and Raman intensities of the vibrations were obtained too. For the more stable species, they are reported in Table VII. Although quantitative agreement with experiment is somewhat illusory at this level of theory, the qualitative features are known to be reproduced quite well.²⁸

For determining the relative stabilities of the several isomers, full fourth-order Møller–Plesset theory²⁹ was applied to these structures using the 6-31G* basis set. In order to reduce the effects of spin contamination, the projected unrestricted Møller–Plesset method (PMP) of Schlegel³⁰ was applied, by which only the next higher spin state is annihilated (i.e., single annihilation). For the PMP4 result, the extrapolation formula suggested by Schlegel was used:

$$E_{\text{PMP4}} \approx E_{\text{UMP4}} + E_{\text{PMP3}} - E_{\text{UMP3}}. \quad (1)$$

In order to obtain an idea of the effect of higher-order terms, the Aitken-type extrapolation of Pople *et al.*³¹ was used too:

$$E_\infty \approx \frac{E_2 + E_3}{1 - E_4/E_2}. \quad (2)$$

The total energies at the various levels are reported in Table I, the dissociation energies for the hypothetical motionless state are found in Table II.

The Hartree–Fock wave function was always tested for internal instability.³² If any such instability was found, a search along the direction of instability was carried out and the wave function reoptimized using a steepest-descent direct minimization method.³³ In a number of cases, this resulted in wave functions not belonging to any irreducible representation of the molecular point group. If such an event occurred, the wave function was constrained to the proper point group symmetry anyway. This decision was justified on empirical grounds by Farnell *et al.*³⁴; in the same paper, it was also shown that the problem was strongly related to basis set incompleteness. Where investigated, the asymmetric wave function always yielded markedly higher post-Hartree–Fock energies than the symmetric one: this conclusion is in complete agreement with Farnell *et al.*

TABLE I. Molecular energies (hartree) of the different boron, nitrogen, and boron–nitrogen species.

Species	3-21G			6-31G*							
	UHF	UHF	UMP2	UMP3	UMP4	PUHF	PMP2	PMP3	PMP4	UMP _{strp}	PMP _{strp}
B(² P)	-24.389 76	-24.522 04	-24.558 72	-24.570 97	-24.575 94	-24.523 72	-24.559 47	-24.571 25	-24.576 23	-24.578 65	-24.578 94
N(⁴ S)	-54.105 39	-54.385 44	-54.457 01	-54.470 65	-54.473 26	-54.386 51	54.457 65	-54.470 99	-54.473 60	-54.473 87	-54.474 20
B ₂ (³ Σ _g ⁻)	N/A	-45.075 34	-49.217 04	-49.239 07	-49.256 97	-49.076 87	-49.218 01	-49.239 63	-49.257 52	-49.262 74	-49.263 26
B ₂ (³ Σ _u ⁻)	N/A	-49.157 84	-49.235 14	-49.249 67	-49.254 84	-49.157 93	-49.235 19	-49.249 70	-49.254 86	-49.256 25	-49.256 27
BN(³ Π)	N/A	-78.990 16	-79.167 92	-79.180 92	-79.192 25	-78.992 81	-79.170 19	-79.182 64	-79.193 97	-79.193 91	-79.195 59
BN(¹ Σ ⁺)	N/A	-78.882 62	-79.168 98	-79.138 51	-79.206 72	-78.882 62	-79.168 98	-79.138 51	-79.206 72	-79.218 52	-79.218 52
N ₂	N/A	-108.943 95	-109.248 19	-109.245 34	-109.266 49	-108.943 95	-109.248 19	-109.245 34	-109.266 49	-109.267 85	-109.267 85
B003	-73.327 24	-73.735 15	-73.904 62	-73.926 23	-73.942 96	-73.733 14	-73.902 58	-73.924 17	-73.940 89	-73.947 15	-73.945 09
B004	-73.344 38	-73.749 98	-73.923 46	-73.943 92	-73.961 00	-73.751 16	-73.924 20	-73.944 37	-73.961 46	-73.965 10	-73.965 54
B004'	N/A	-73.761 53	-73.904 52	-73.929 33	-73.942 86	-73.762 69	-73.905 69	-73.930 44	-73.943 97	-73.946 87	-73.947 97
B005	-73.337 62	-73.772 07	-73.966 19	-73.986 39	-74.011 57	-73.799 33	-73.992 18	-74.009 29	-74.034 47	-74.018 33	-74.040 82
B006	-73.335 25	-73.762 26	-73.924 71	-73.948 46	-73.963 92	-73.767 59	-73.929 81	-73.952 94	-73.968 40	-73.968 04	-73.972 46
B008	-73.338 26	-73.764 46	-73.929 87	-73.953 43	-73.969 33	-73.769 07	-73.934 26	-73.957 19	-73.973 09	-73.973 53	-73.977 22
B010	-73.327 56	-73.754 90	-73.917 62	-73.941 58	-73.957 73	-73.761 08	-73.923 52	-73.946 73	-73.962 87	-73.962 15	-73.967 22
BN007	-103.082 48	-103.649 80	-103.856 19	-103.882 24	-103.898 00	-103.689 16	-103.895 04	-103.920 03	-103.935 78	-103.901 45	-103.939 16
BN007'	N/A	-103.603 68	-103.787 96	-103.815 89	-103.824 94	-103.605 46	-103.789 04	-103.816 48	-103.825 53	-103.826 85	-103.827 42
BN008	-103.045 28	-103.618 69	-103.827 97	-103.852 45	-103.866 78	-103.625 63	-103.834 47	-103.857 95	-103.872 28	-103.869 64	-103.875 07
BN009	-103.105 89	-103.673 88	-103.970 65	-103.977 68	-104.008 14	-103.678 10	-103.973 31	-103.979 11	-104.009 57	-104.012 43	-104.013 75
BN010	-103.104 91	-103.674 71	-103.906 26	-103.916 39	-103.932 12	-103.683 35	-103.913 48	-103.921 65	-103.937 37	-103.934 00	-103.939 13
BN012	-103.050 41	-103.654 25	-103.914 38	-103.921 07	-103.939 71	-103.657 26	-103.916 66	-103.922 62	-103.941 25	-103.941 66	-103.943 16
BN003	-132.693 12	-133.448 99	-133.796 35	-133.811 23	-133.837 53	-133.457 06	-133.802 92	-133.815 86	-133.842 06	-133.840 89	-133.845 27
BN003'	N/A	-133.455 91	-133.788 17	-133.801 64	-133.827 04	-133.474 20	-133.805 81	-133.818 11	-133.843 51	-133.830 26	-133.846 63
BN004	-132.731 61	-133.484 55	-133.792 89	-133.807 09	-133.827 89	-133.500 67	-133.806 18	-133.816 54	-133.837 34	-133.830 43	-133.839 62
BN005	N/A	-133.375 73	-133.768 66	-133.763 40	-133.826 00	-133.392 74	-133.782 38	-133.771 71	-133.834 31	-133.836 86	-133.844 25
BN005'	N/A	-133.393 43	-133.730 17	-133.745 15	-133.778 66	-133.431 91	-133.765 91	-133.775 57	-138.809 09	-133.784 02	-133.813 90
BN006	-132.733 87	-133.469 89	-133.743 37	-133.773 32	-133.789 14	-133.483 79	-133.755 11	-133.782 05	-133.797 87	-133.791 95	-133.800 52
BN011	N/A	-133.459 13	-133.818 91	-133.824 92	-133.847 48	-133.460 43	-133.819 86	-133.825 62	-133.848 17	-133.849 39	-133.850 07
BN013	-132.647 32	-133.430 89	-133.794 29	-133.804 09	-133.830 94	-133.434 75	-133.796 58	-133.805 24	-133.832 09	-133.833 86	-133.834 93
BN014	-132.624 32	-133.404 03	-133.747 91	-133.753 92	-133.778 20	-133.410 77	-133.752 86	-133.756 94	-133.781 22	-133.780 51	-133.783 39
N003	-162.206 04	-163.180 59	-163.602 28	-163.615 93	-163.645 60	-163.205 37	-163.624 30	-163.632 75	-163.662 42	-163.648 87	-163.665 32
N004	-162.039 97	-163.959 53	-163.430 01	-163.425 00	-163.467 21	-163.966 66	-163.434 21	-163.426 74	-163.468 94	-163.470 88	-163.472 39
N005	-162.213 59	-163.196 68	-163.623 66	-163.636 13	-163.666 18	-163.219 30	-163.643 32	-163.650 41	-163.680 46	-163.669 40	-163.683 30
N006	-162.145 25	-163.098 95	-163.513 09	-163.524 20	-163.552 41	-163.107 03	-163.518 05	-163.526 71	-163.554 91	-163.555 28	-163.557 63
N007	N/A	-163.191 93	-163.642 79	-163.648 36	-163.676 36	-163.196 51	-163.646 15	-163.650 53	-163.678 54	-163.678 59	-163.680 69
N008	-162.169 89	-163.098 46	-163.501 67	-163.515 80	-163.543 53	-163.106 43	-163.506 80	-163.518 67	-163.546 40	-163.546 62	-163.549 34
N009	-162.289 27	-163.245 80	-163.686 87	-163.689 89	-163.724 16	-163.262 93	-163.700 52	-163.698 45	-163.732 72	-163.727 31	-163.735 46
N010	-162.242 86	-163.157 34	-163.521 46	-163.545 05	-163.570 55	-163.174 91	-163.536 44	-163.556 19	-163.581 69	-163.574 24	-163.585 12
N010'	N/A	-163.244 28	-163.599 20	-163.624 79	-163.648 33	-163.263 24	-163.615 46	-163.637 07	-163.660 61	-163.651 82	-163.663 84

The spin projection proved invaluable in this study. Nevertheless, it breaks down in some cases, or does not annihilate the contamination satisfactorily. Since the convergence of the Møller–Plesset series is very sensitive towards spin contamination,³⁵ coupled-cluster calculations were carried out for the most stable isomers of each species, using the CCD + ST(CCD) procedure of Raghavachari.³⁶ This method was applied in order to obtain a more reliable picture of the mutual separations, since the coupled cluster method is nowhere near as sensitive towards spin contamination as many-body perturbation theory. Actually, the CCSD energy can be proven to be invariant towards projection of any single spin contaminant.³⁷ The results are presented in Table V.

III. RESULTS AND DISCUSSION

An overview of the stationary points for the B₃, B₂N, BN₂, and N₃ clusters at the UHF/6-31G* level can be found in Figs. 1–4. The relevant geometrical parameters are also indicated in these figures. The molecular energies, binding energies, and electronic configurations of the clusters under

study are given in Tables I, II, and III, respectively. [In the subsequent discussion, the term “binding energy” will always refer to the molecule in a hypothetical motionless state (i.e., no zero-point vibration), contrary to the “dissociation energy,” where the zero-point vibration is included.] The point groups, electronic states, and expectation values for S² are presented in the latter table. The UHF/6-31G* harmonic frequencies and the zero-point energies are collected in Table IV. The Mulliken charge distributions³⁸ at the UHF/6-31G* level for the most important clusters are presented in Fig. 5. For the most stable species, the first vertical ionization potentials obtained by applying Koopmans’ theorem³⁹ to the UHF/6-31G* wave function are presented in the relevant portions of the text. Such ionization potentials are known to be generally in satisfactory agreement with experiment⁴⁰ when a basis set of at least double-zeta quality is used.

A. Diatomic clusters B₂, BN, and N₂

These clusters are discussed here for two reasons (i) to assess the quality of our theoretical model for these species;

TABLE II. Molecular binding energies (kcal mol⁻¹) of the boron, nitrogen, and boron–nitrogen species.

Species	3-21G			6-31G*							
	UHF	UHF	UMP2	UMP3	UMP4	PUHF	PMP2	PMP3	PMP4	UMP _{xip}	PMP _{xip}
B clusters											
B ₂ (³ Σ _g ⁻)	N/A	19.62	62.50	60.96	65.94	18.47	62.17	60.95	65.93	66.16	66.13
B ₂ (⁵ Σ _u ⁻)	N/A	71.39	73.86	67.61	64.60	69.34	72.95	67.27	64.26	62.09	61.75
B003	99.12	106.08	143.37	133.87	134.99	101.65	140.67	132.05	133.17	132.53	130.69
B004	109.88	115.38	155.18	144.97	146.31	112.96	154.24	144.72	146.07	143.80	143.53
B004'	N/A	122.63	143.30	135.82	134.93	120.19	142.62	135.98	135.10	132.35	132.50
B005	105.64	129.24	182.00	171.62	178.05	143.18	196.90	185.46	191.89	177.20	190.77
B006	104.15	123.08	155.97	147.82	148.15	123.26	157.76	150.10	150.43	145.64	147.87
B008	106.04	124.47	159.21	150.94	151.54	124.19	160.55	152.76	153.37	149.08	150.86
B010	99.32	118.47	151.52	143.50	144.26	119.18	153.81	146.20	146.96	141.94	144.58
BN clusters											
BN(³ Π)	N/A	51.88	95.50	87.42	89.77	51.82	96.06	88.10	90.45	88.72	89.39
BN(¹ Σ ⁺)	N/A	-15.60	96.17	60.80	98.84	-17.33	95.29	60.41	98.45	104.16	103.77
BN007	123.98	138.23	176.80	169.21	171.22	160.15	199.84	192.36	194.36	169.60	192.70
BN007'	N/A	109.29	133.98	127.57	125.37	107.63	133.32	127.38	125.17	122.79	122.58
BN008	100.63	118.71	159.09	150.52	151.63	120.28	161.83	153.40	154.51	149.64	152.48
BN009	138.66	153.34	248.62	229.10	240.34	153.21	248.95	229.43	240.67	239.25	239.50
BN010	138.05	153.86	208.22	190.64	192.63	156.50	211.41	193.37	195.36	190.03	192.68
BN012	103.85	141.02	213.31	193.58	197.39	140.13	213.40	193.98	197.79	194.84	195.21
BN003	58.10	97.94	203.07	187.66	197.71	100.60	205.92	189.90	199.95	197.35	199.50
BN003'	N/A	102.28	197.94	181.59	191.13	111.36	207.73	191.31	200.86	190.68	200.36
BN004	82.24	120.25	200.90	185.00	191.66	127.97	207.96	190.33	196.99	190.79	195.96
BN005	N/A	51.97	185.70	157.59	190.47	60.24	193.03	162.20	195.09	194.82	198.86
BN005'	N/A	63.07	161.55	146.13	160.77	84.82	182.70	164.62	179.26	161.66	179.82
BN006	83.66	111.05	169.82	163.81	167.35	117.37	175.92	168.69	172.22	166.64	171.42
BN011	N/A	104.30	217.23	196.19	203.95	102.72	216.55	196.03	203.78	202.68	202.51
BN013	29.36	86.58	201.78	183.12	193.58	86.60	201.94	183.24	193.69	192.94	193.01
BN014	14.92	69.72	172.67	151.64	160.48	71.56	174.51	152.93	161.77	159.46	160.67
N clusters											
N ₂	N/A	108.60	209.70	190.78	200.79	107.26	208.89	190.36	200.36	200.87	200.46
N003	-69.11	15.22	145.11	128.00	141.71	28.76	157.73	137.91	151.62	142.61	152.30
N004	-173.32	-123.49	37.01	8.19	29.77	-121.03	38.44	8.63	30.21	30.92	31.24
N005	-64.37	25.32	158.53	140.67	154.63	37.51	169.66	148.99	162.95	155.49	163.58
N006	-107.25	-36.00	89.15	70.44	83.23	-32.95	91.06	71.37	84.16	83.88	84.73
N007	N/A	22.34	170.53	148.35	161.01	23.21	171.44	149.07	161.74	161.25	161.95
N008	-91.79	-36.31	81.98	65.16	77.66	-33.32	84.00	66.32	78.82	78.44	79.53
N009	-16.88	56.14	198.20	174.41	191.01	64.88	205.56	179.13	195.74	191.83	196.32
N010	-46.00	0.64	94.40	83.52	94.61	9.65	102.60	89.87	100.96	95.78	101.98
N010'	N/A	55.19	143.18	133.56	143.43	65.08	152.19	140.62	150.49	144.46	151.38

(ii) to obtain the data necessary in the thermochemical analysis for the larger clusters.

It is quickly seen, that only at the MP4 level of MBPT, the correct ground state for B₂ is predicted; a similar observation was made by Raghavachari³⁶ with the much larger 6-311 + G(3df) basis set.⁴¹ At the MP4 and PMP4 levels, ³Σ_g⁻ – ⁵Σ_u⁻ splittings of only 1.34 and 1.67 kcal mol⁻¹, respectively, are found. When extrapolation for higher order effects is performed, this rises to 4.07 and 4.38 kcal mol⁻¹ for the unprojected and projected methods, respectively. CCD calculations yielded the wrong ground state (again in agreement with Raghavachari), whereas CCD + ST(CCD) yields 2.09 kcal mol⁻¹ for the splitting. The best theoretical value using a very large STO basis set and MCSCF/MRCI methods, is 3.6 kcal mol⁻¹ [Ref. 14(a)], whereas Raghavachari found 3.3 kcal mol⁻¹ at the CCD + ST(CCD)/6-311 + G(3df) level.

For the low-lying ¹Σ⁺ excited state of BN, the MP series exhibits oscillation; so does the predicted ground state. Henceforth, only the coupled cluster values are in any way

reliable. CCD predicts the correct ground state (³Π), but gives an exaggerated value for the ¹Σ⁺ – ³Π splitting: CCD + ST(CCD) yields 4.25 kcal mol⁻¹, in qualitative agreement with the Karna and Grein MRD-CI/DZP result of 0.1 eV.

If one looks at the binding energies of B₂ and N₂ (for BN no experimental data are available), it can be seen that they are all underestimated. Experimental data (Huber and Herzberg, corrected for zero-point energy) are 3.08 eV (± about 0.1 eV) for B₂, and 9.90 eV for N₂ (from a very accurate dissociation energy). CCD + ST(CCD) yields 2.74 and 8.62 eV, whereas PMP extrapolated for higher order effects yields 2.87 and 8.69 eV, respectively. In other words, CCD + ST(CCD)/6-31G* recovers 89.5% and 87%, respectively, of the binding energies. A similar observation was made by Raghavachari and Binkley,¹² who found that the same theoretical model recovered ~90% of the binding energies for C₂ and C₃, and suggested that the calculated binding energies be scaled by 1.1, yielding excellent agreement with the available experimental data for C₂ to C₇. A similar

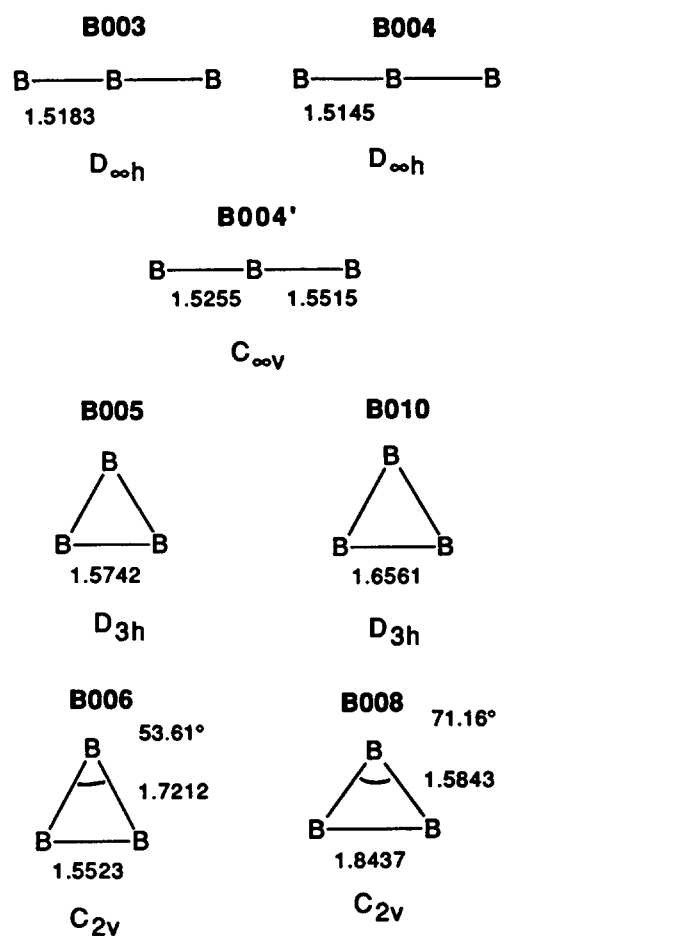


FIG. 1. Stationary points (UHF/6-31G*) for B_3 . Bond distances in Ångstrom units.

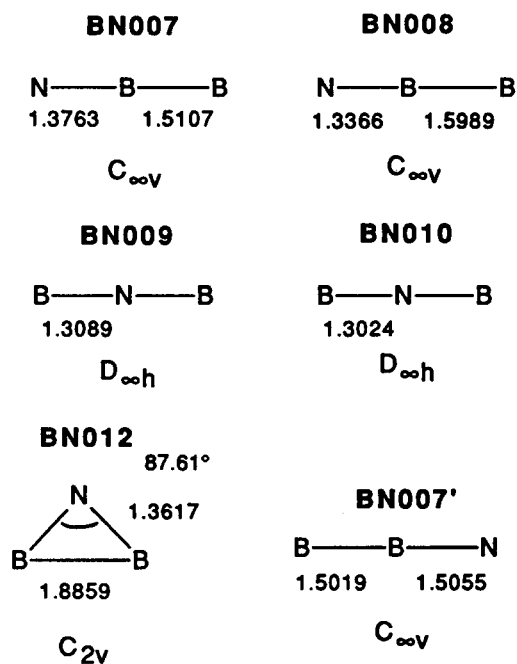


FIG. 2. Stationary points (UHF/6-31G*) for B_2N . Bond distances in Ångstrom units.

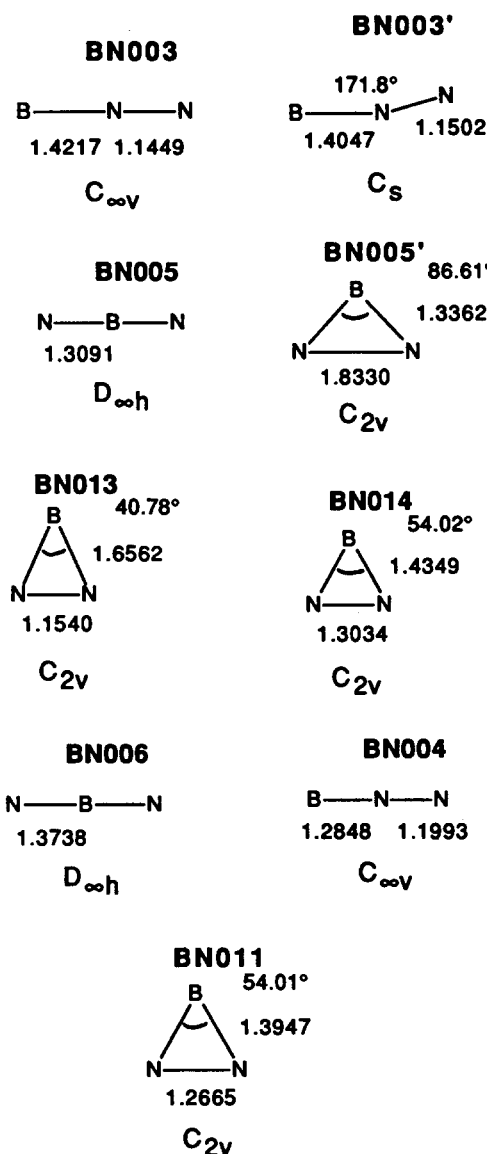


FIG. 3. Stationary points (UHF/6-31G*) for BN_2 . Bond distances in Ångstrom units.

argument was presented in a study of silicon clusters.⁴² Following the same lines, we suggest that our calculated $\text{CCD} + \text{ST}(\text{CCD})/6\text{-}31\text{G}^*$ binding energies be scaled by 1.15, yielding the values 3.15 and 9.91 eV for B_2 and N_2 , respectively, in excellent agreement with experiment. For the molecules under study here, we estimate (by analogy with the carbon and silicon cluster results) that binding energies estimated in this way will be off by at most 0.2 eV (actual errors for the three-membered clusters will rather be on the order of 0.1 eV, or about 2 kcal mol⁻¹). At 4000 K, an error of 0.2 eV signifies an error on log K of 0.25 only, so binding energies estimated in this way should be of some value.

From scaling by 1.15, we can then predict here a binding energy of 101.9 kcal mol⁻¹ for BN or a dissociation energy of 99.6 kcal mol⁻¹. This is in agreement with an extrapolation from the spectroscopic data by Gaydon⁴³ of 4.0 ± 0.5 eV, or 92 ± 12 kcal mol⁻¹. Other values of 5.7 and 6.2 eV,⁴⁴

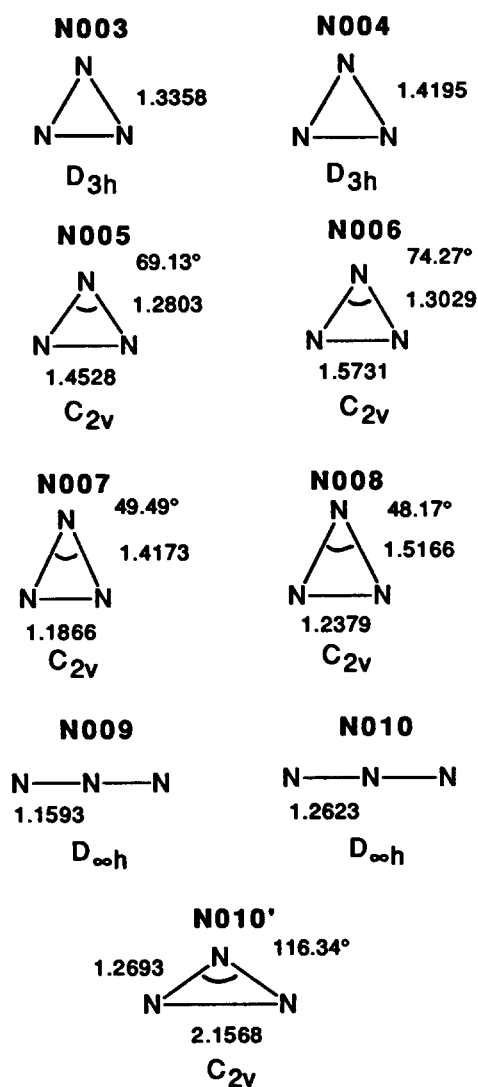


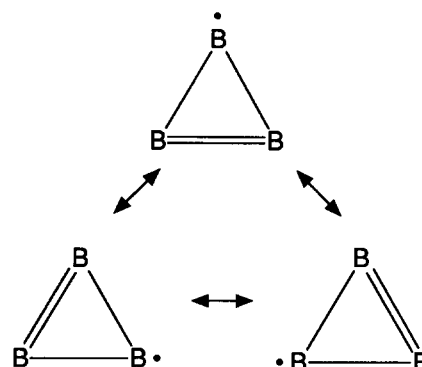
FIG. 4. Stationary points (UHF/6-31G*) for N_3 . Bond distances in Ångstrom units.

as well as estimates of 5.4, 5.6, 6.0, and 6.4 eV³⁹ based on parent molecules seem to be in error.

B. B_3

At the 3-21G level, the linear quartet B004 would be lowest in energy (see Table I), while it is actually a transition state towards deformation to the $C_{\infty v}$ structure. On the contrary, at the 6-31G* level, the equilateral triangle B005 sinks below B004 by no less than 14 kcal mol⁻¹. The other cyclic structures are also lowered quite a lot in energy. This observation is in agreement with the known fact,⁴⁵ that polarization functions are required for an adequate description of strained rings. At the UHF/6-31G* level, B005 is only slightly below the quartet structure B008. At the Møller–Plesset level, on the other hand, the separation is much enlarged. The same happens when spin projection is performed. Finally, at the highest level of theory indicated in this table, the equilateral triangle B005 markedly comes out as the most stable structure. The separation with its lowest neighbor amounts to 39.9 kcal mol⁻¹, which still gives rise

to an isomerization equilibrium constant of about 150 even at 4000 K. The differences in partition functions are not capable of changing this conclusion significantly. Henceforth, the equilibrium structure of B_3 can be taken as B005 for all intents and purposes. It is stabilized by resonance:



A further glance at the potential surface of the doublet state yields the linear structure B003 as the other minimum, situated 60.1 kcal mol⁻¹ above the ground state (B005). B003 has an extremely low bending frequency (101.5 cm⁻¹ after scaling by 0.89, as suggested by Pople *et al.*⁴⁶), in which it parallels the theoretical⁴⁷ and experimental⁴⁸ behavior of C_3 . Because of this, it may be expected not to have an appreciable lifetime, if ever formed. An isosceles triangle with an apex angle greater than 60 deg may be expected as the transition state between B003 and B005.

The situation is a little different for the quartet state. The isosceles triangle B010 is a Jahn–Teller crossing, deforming towards the isosceles triangle B008 having an apex angle of 71.16 deg. The structure B006, with apical angle 53.61 deg corresponds to three equivalent transition states connecting three equivalent local minima with structure B008 on the Jahn–Teller surface via C_s intermediate structures. B004 is a transition state towards deformation to an asymmetric ($C_{\infty v}$) linear structure B004'. At all correlated levels, however, this structure is distinctly higher in energy than B004, so the deformation must be regarded as an artifact of the optimization level.

Summing up, the equilibrium structure of B_3 may unambiguously be predicted as an equilateral triangle with term symbol $^2A'_1$ and spectroscopic parameters predicted at this level as: bond distance of 1.574 Å, harmonic frequencies 1083 cm⁻¹ (A'_1 , medium/strong Raman) and 865 cm⁻¹ (E' , medium/strong IR). From the scaled CC procedure (vide supra), the binding energy is predicted to be 202.0 kcal mol⁻¹; together with the zero-point energy, this yields a dissociation energy of 197.9 kcal mol⁻¹. The vertical ionization potential according to Koopmans' theorem (at the UHF/6-31G* level is 9.52 eV (a'_2 orbital, leading to a $^3A'_2$ state for the ion).

C. B_2N

At the 3-21G level, the two symmetric linear structures BN009 and BN010 are the most stable ones, with a difference of only 0.5 kcal mol⁻¹. The asymmetric linear doublet BN007 follows 14.5 kcal mol⁻¹ higher. At the 6-31G* level,

TABLE III. Electronic configurations and expectation values for S^2 .

Species	Formula	Point group	Term	$\langle S^2 \rangle^a$	$\langle S^2 \rangle^b$	$\langle S^2 \rangle^c$	Electronic configuration
B ₂	B ₂	$D_{\infty h}$	$^3\Sigma_g^-$	2.011	2.003	2.000	$(\sigma_g)^2(\sigma_u)^2(\sigma_g)^2(\sigma_u)^2(\pi_u)^2$
B ₂	B ₂	$D_{\infty h}$	$^5\Sigma_u^-$	6.001	6.000	6.000	$(\sigma_g)^2(\sigma_u)^2(\sigma_g)^2(\sigma_u)(\sigma_g)(\pi_u)^2$
BN	BN	$C_{\infty v}$	$^3\Pi$	2.043	2.031	2.000	$(\sigma)^2(\sigma)^2(\sigma)^2(\sigma)^2(\pi)^3(\sigma)$
BN	BN	$C_{\infty v}$	$^1\Sigma^+$	0.000	0.000	0.000	$(\sigma)^2(\sigma)^2(\sigma)^2(\sigma)^2(\pi)^4$
N ₂	N ₂	$D_{\infty h}$	$^1\Sigma_g^+$	0.000	0.000	0.000	$(\sigma_g)^2(\sigma_u)^2(\sigma_g)^2(\sigma_u)^2(\sigma_g)^2(\pi_u)^4$
B003	B ₃	$D_{\infty h}$	$^2\Pi_g$	1.775	1.801	0.834	$(\sigma_g)^2(\sigma_u)^2(\sigma_g)^2(\sigma_u)^2(\sigma_g)(\sigma_u)(\pi_u)^3$
B004	B ₃	$D_{\infty h}$	$^4\Pi_g$	3.759	3.752	3.750	$(\sigma_g)^2(\sigma_u)^2(\sigma_g)^2(\sigma_u)^2(\sigma_g)(\sigma_u)(\pi_u)^3$
B004'	B ₃	$C_{\infty v}$	$^4\Pi$	4.392	4.395	3.759	$(\sigma)^2(\sigma)^2(\sigma)^2(\sigma)^2(\sigma)^2(\sigma)(\pi)^3$
B005	B ₃	D_{3h}	$^2A'_1$	1.542	1.441	1.193	$(a'_1)^2(e')^4(a'_1)^2(e')^4(a'_1)(a'_2)^2$
B006	B ₃	C_{2v}	4B_1	4.115	4.084	3.754	$(a_1)^2(a_1)^2(b_2)^2(a_1)^2(a_1)^2(b_2)^2(a_1)(b_1)(a_1)$
B008	B ₃	C_{2v}	4A_2	4.050	4.022	3.755	$(a_1)^2(b_2)^2(a_1)^2(a_1)^2(b_2)^2(a_1)^2(a_1)(b_1)(b_2)$
B010	B ₃	D_{3h}	4 fuzzy	4.139	4.103	3.762	fuzzy symmetry
BN007	B ₂ N	$C_{\infty v}$	$^2\Sigma^+$	2.315	2.231	2.621	$(\sigma)^2(\sigma)^2(\sigma)^2(\sigma)^2(\sigma)^2(\sigma)^2(\pi)^4$
BN007'	B ₂ N	$C_{\infty v}$	$^6\Sigma^+$	8.763	8.753	8.750	$(\sigma)^2(\sigma)^2(\sigma)^2(\sigma)^2(\sigma)^2(\sigma)^2(\pi)^2(\sigma)(\pi)^2$
BN008	B ₂ N	$C_{\infty v}$	$^4\Sigma^+, \Sigma^-, \Delta$	4.046	4.008	3.753	$(\sigma)^2(\sigma)^2(\sigma)^2(\sigma)^2(\sigma)^2(\sigma)^2(\pi)^3(\sigma)(\pi)$
BN009	B ₂ N	$D_{\infty h}$	$^2\Sigma_u^-$	0.776	0.757	0.750	$(\sigma_g)^2(\sigma_u)^2(\sigma_g)^2(\sigma_u)^2(\sigma_u)^2(\pi_u)^4(\sigma_g)^2(\sigma_u)$
BN010	B ₂ N	$D_{\infty h}$	$^4\Pi_u$	3.924	3.866	3.754	$(\sigma_g)^2(\sigma_u)^2(\sigma_g)^2(\sigma_u)^2(\sigma_u)^2(\sigma_g)^2(\pi_u)^4(\sigma_u)(\pi_g)$
BN012	B ₂ N	C_{2v}	4B_2	3.787	3.769	3.750	$(a_1)^2(a_1)^2(b_2)^2(a_1)^2(a_1)^2(b_2)^2(a_1)(b_1)^2(b_2)(a_1)$
BN003	BN ₂	$C_{\infty v}$	$^2\Pi$	0.818	0.792	0.753	$(\sigma)^2(\sigma)^2(\sigma)^2(\sigma)^2(\sigma)^2(\sigma)^2(\pi)^4(\sigma)^2(\pi)$
BN003'	BN ₂	C_s	$^2A''$	1.345	1.296	0.899	$(a')^2(a')^2(a')^2(a')^2(a')^2(a')^2(a')^2(a'')^2(a')^2(a')^2(a'')$
BN004	BN ₂	$C_{\infty v}$	$^4\Sigma^-$	3.991	3.901	3.769	$(\sigma)^2(\sigma)^2(\sigma)^2(\sigma)^2(\sigma)^2(\sigma)^2(\pi)^4(\sigma)(\pi)^2$
BN005	BN ₂	$D_{\infty h}$	$^2\Pi_g$	0.909	0.846	0.755	$(\sigma_g)^2(\sigma_u)^2(\sigma_g)^2(\sigma_u)^2(\sigma_u)^2(\sigma_g)^2(\pi_u)^4(\sigma_u)^2(\pi_g)$
BN005'	BN ₂	C_{2v}	2A_2	1.416	1.293	1.085	$(a_1)^2(b_2)^2(a_1)^2(a_1)^2(b_2)^2(a_1)^2(b_1)^2(b_2)^2(a_1)^2(a_2)$
BN006	BN ₂	$D_{\infty h}$	$^4\Pi_u$	4.005	3.925	3.755	$(\sigma_u)^2(\sigma_g)^2(\sigma_u)^2(\sigma_g)^2(\sigma_u)^2(\sigma_g)^2(\pi_u)^3(\sigma_u)^2(\pi_g)^2$
BN011	BN ₂	C_{2v}	2A_1	0.760	0.754	0.750	$(a_1)^2(b_2)^2(a_1)^2(a_1)^2(b_2)^2(a_1)^2(a_1)^2(b_1)^2(b_2)^2(a_1)$
BN013	BN ₂	C_{2v}	2B_2	0.763	0.752	0.750	$(a_1)^2(b_2)^2(a_1)^2(a_1)^2(b_2)^2(a_1)^2(a_1)^2(b_1)^2(b_2)(a_1)^2$
BN014	BN ₂	C_{2v}	4B_1	3.811	3.778	3.751	$(a_1)^2(b_2)^2(a_1)^2(a_1)^2(b_2)^2(a_1)^2(b_1)^2(a_1)^2(a_1)(b_2)(a_2)$
N003	N ₃	D_{3h}	2 fuzzy	1.078	1.003	0.766	fuzzy symmetry
N004	N ₃	D_{3h}	$^4A'_1$	3.788	3.756	3.751	$(e')^4(a'_1)^2(a'_1)^2(e')^4(e')^4(a'_1)(e'')$
N005	N ₃	C_{2v}	2A_2	1.009	0.940	0.759	$(a_1)^2(a_1)^2(b_2)^2(a_1)^2(b_2)^2(a_1)^2(b_1)^2(a_1)^2(b_2)(a_1)^2(a_2)$
N006	N ₃	C_{2v}	4B_2	3.794	3.760	3.751	$(a_1)^2(b_2)^2(a_1)^2(a_1)^2(b_2)^2(a_1)^2(b_1)^2(a_1)^2(b_2)(a_1)(a_2)(b_1)$
N007	N ₃	C_{2v}	2B_1	0.772	0.760	0.750	$(a_1)^2(b_2)^2(a_1)^2(a_1)^2(b_2)^2(b_1)^2(a_1)^2(a_1)^2(b_2)^2(b_1)$
N008	N ₃	C_{2v}	4A_1	3.798	3.763	3.751	$(a_1)^2(a_1)^2(b_2)^2(a_1)^2(a_1)^2(b_2)^2(b_1)^2(a_1)^2(b_2)(b_1)(a_2)$
N009	N ₃	$D_{\infty h}$	$^2\Pi_g$	0.881	0.827	0.754	$(\sigma_g)^2(\sigma_u)^2(\sigma_g)^2(\sigma_u)^2(\sigma_u)^2(\sigma_g)^2(\pi_u)^4(\sigma_u)^2(\pi_g)^3$
N010	N ₃	$D_{\infty h}$	$^4\Pi_g$	4.047	3.957	3.760	$(\sigma_u)^2(\sigma_g)^2(\sigma_u)^2(\sigma_g)^2(\sigma_u)^2(\sigma_g)^2(\pi_u)^4(\sigma_u)^2(\pi_g)^2(\pi_g)$
N010'	N ₃	C_{2v}	4B_1	4.061	3.970	3.761	$(a_1)^2(a_1)^2(b_2)^2(a_1)^2(b_2)^2(a_1)^2(b_1)^2(b_2)^2(a_1)^2(b_2)(a_1)$

^a For UHF wave function.

^b For first-order MBPT wave function.

^c For spin-projected UHF wave function.

on the other hand, the bent quartet BN012 is found most stable, in agreement with the earlier remarks about the effect of polarization functions. A bent doublet structure was not found as a stationary point.

Spin projection results in a marked stabilization of BN007. Inspection of $\langle S^2 \rangle$ reveals an excessive amount of spin contamination: annihilation of the first contaminant actually increases, rather than decreases, spin contamination. This suggests that strong contamination by states with even higher multiplicity (sextuplets, octuplets) is present. Because of the B–B–N structure, and given the fact that B₂ is known to have a very low-lying $^5\Sigma_u^-$ state besides the ground $^3\Sigma_g^-$ state, this observation is explainable from a diatomics-in-molecules viewpoint: the sextuplets follow naturally from connecting the $^5\Sigma_u^-$ B₂ to the 4S nitrogen atom. Indeed, a

$^6\Sigma^+$ state BN007' was found to lie only 28.9 kcal mol⁻¹ above the doublet state at the Hartree–Fock level: given the high value of S^2 for a sextuplet (8.75 exact, 8.763 for BN007'), the above explanation seems plausible.

When electron correlation is taken into account, BN009 markedly sinks below the other states, because of the stronger dynamic correlation effects in a doublet as opposed to the corresponding quartet. (The Fermi correlation between electrons of like spin is already accounted for by the Hartree–Fock model⁴⁹). For the sextuplets contaminating BN007, the dynamic correlation would be even smaller. Indeed, BN007' lies 45.8 kcal mol⁻¹ above BN007 at the UMP4 level, and 69.2 kcal mol⁻¹ at the PMP4 level. The lowest-lying excited structure would be the bent BN012, 44.3 kcal mol⁻¹ higher in energy. BN007 and BN010 are

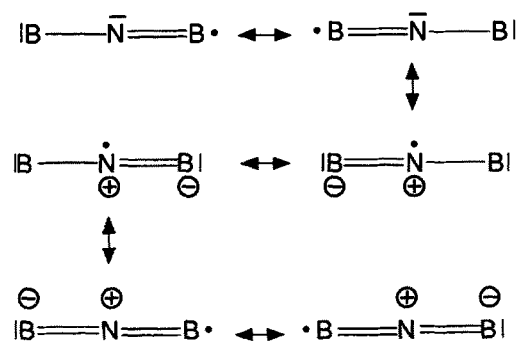
TABLE IV. Point group, term, normal modes, and zero point energy.

Species	Formula	Point group	Term	ν_4 (cm^{-1})	ν_3 (cm^{-1})	ν_2 (cm^{-1})	ν_1 (cm^{-1})	E_{zp} (kcal mol^{-1})
Diatomic species								
B ₂	B ₂	$D_{\infty h}$	$^3\Sigma_g^-$				1086 Σ_g	1.55
B ₂	B ₂	$D_{\infty h}$	$^5\Sigma_u^-$				1395 Σ_g	1.99
BN	BN	$C_{\infty v}$	$^1\Sigma^+$				1890 Σ	2.70
BN	BN	$C_{\infty v}$	$^3\Pi$				1767 Σ	2.53
N ₂	N ₂	$D_{\infty h}$	$^1\Sigma_g^+$				2758 Σ_g	3.94
B ₃ isomers								
B003	B ₃	$D_{\infty h}$	$^2\Pi_g$	89.1 Π_u	139 Π_u	965 Σ_g	1574 Σ_u	3.96
B004	B ₃	$D_{\infty h}$	$^4\Pi_g$	541 <i>i</i> Σ_u	131 Π_u	193 Π_u	958 Σ_g	1.83
B004'	B ₃	$C_{\infty v}$	$^4\Pi$	241 Π	369 Π	878 Σ	1266 Σ	3.94
B005	B ₃	D_{3h}	$^2A_1'$		972 E'	972 E'	1217 A_1'	4.52
B006	B ₃	C_{2v}	4B_1		518 <i>i</i> B_2	888 A_1	1230 A_1	3.03
B008	B ₃	C_{2v}	4A_2		523 A_1	756 B_2	1113 A_1	3.42
B010	B ₃	D_{3h}	$^4\text{fuzzy}$		1532 <i>i</i> ??	776 ??	1112 ??	2.70
B ₂ N and BN ₂ isomers								
BN007	B ₂ N	$C_{\infty v}$	$^2\Sigma^+$	302 Π	302 Π	927 Σ	1616 Σ	4.50
BN007'	B ₂ N	$C_{\infty v}$	$^6\Sigma^+$	370 Π	370 Π	857 Σ	1541 Σ	4.49
BN008	B ₂ N	$C_{\infty v}$	$^4\Sigma^+, \Sigma^-, \Delta$	270 Π	394 Π	879 Σ	1257 Σ	4.00
BN009	B ₂ N	$D_{\infty h}$	$^2\Sigma_u^+$	82 Π_u	82 Π_u	1245 Σ_g	2271 Σ_u	5.26
BN010	B ₂ N	$D_{\infty h}$	$^4\Pi_u$	273 Π_u	451 Π_u	1293 Σ_g	1504 Σ_u	5.03
BN012	B ₂ N	C_{2v}	4B_2		786 A_1	1203 B_2	1525 A_1	5.02
BN003	BN ₂	$C_{\infty v}$	$^2\Pi$	114 <i>i</i> Π	287 Π	1016 Σ	2003 Σ	4.72
BN003'	BN ₂	C_s	$^2A''$		305 A''	1051 A'	1822 A'	4.54
BN004	BN ₂	$C_{\infty v}$	$^4\Sigma^-$	461 Π	461 Π	1304 Σ	1619 Σ	5.50
BN005	BN ₂	$D_{\infty h}$	$^2\Pi_g$	945 <i>i</i> Π_u	211 Π_u	1127 Σ_g	1905 Σ_u	4.64
BN005'	BN ₂	C_{2v}	2A_2		1163 <i>i</i> B_2	399 A_1	1376 A_1	2.54
BN006	BN ₂	$D_{\infty h}$	$^4\Pi_u$	269 Π_u	390 Π_u	946 Σ_g	1215 Σ_u	4.03
BN011	BN ₂	C_{2v}	2A_1		1221 B_2	1290 A_1	1760 A_1	6.10
BN013	BN ₂	C_{2v}	2B_2		251 <i>i</i> B_2	732 A_1	2156 A_1	4.13
BN014	BN ₂	C_{2v}	4B_1		193 <i>i</i> B_2	1217 A_1	1538 A_1	3.94
N ₃ isomers								
N003	N ₃	D_{3h}	$^2\text{fuzzy}$		173 <i>i</i> ??	1121 ??	1606 ??	3.90
N004	N ₃	D_{3h}	$^4A_1'$		818 E'	818 E'	1358 A_1'	4.28
N005	N ₃	C_{2v}	2A_2		566 B_2	1024 A_1	1658 A_1	4.64
N006	N ₃	C_{2v}	4B_2		276 <i>i</i> B_2	696 A_1	1563 A_1	3.23
N007	N ₃	C_{2v}	2B_1		985 A_1	2040 A_1	2788 B_2	8.31
N008	N ₃	C_{2v}	4A_1		302 <i>i</i> B_2	543 A_1	1796 A_1	3.34
N009	N ₃	$D_{\infty h}$	$^2\Pi_g$	530 Π_u	679 Π_u	1504 Σ_g	1703 Σ_u	6.31
N010	N ₃	$D_{\infty h}$	$^4\Pi_g$	1019 <i>i</i> Π_u	257 Π_u	1110 Σ_g	1341 Σ_u	3.87
N010'	N ₃	C_{2v}	4B_1		676 A_1	967 B_2	1299 A_1	4.21

about equal in energy at the PMP4 level, both about 47 kcal mol^{-1} above the ground state. Any improved treatment is unlikely to bridge this gap for BN007.

At this level of theory, B₂N is predicted to have a symmetric linear ($D_{\infty h}$) structure with a $^2\Sigma_u^+$ ground state, with the following spectroscopical parameters: bond distance 1.309 Å, harmonic frequencies 2021 cm^{-1} (Σ_u), 1108 cm^{-1} (Σ_g), and 73 cm^{-1} (Π_u). The Σ_u mode is predicted to be extremely intense (Table VII). It has a surprisingly low Koopmans vertical ionization potential of only 6.75 eV (σ_g^+ , leading to a $^3\Sigma_u^+$ state); BN007 is more reluctant at 9.95 eV (π , leading to a $^1\Pi$ state). As can be seen from the Mulliken charge distributions in Fig. 5, BN009 has a very polar character, with a high negative charge on the central nitrogen atom. Concerning the extremely low bending frequency, the analogy with the behavior of C₃ should be noted:

B₂N is isoelectronic with C₃ except for one electron. BN009 is stabilized by resonance:



For the quartet state, the C_{2v} structure BN012 will be most stable. It is isoelectronic with B₃ except for two unpaired

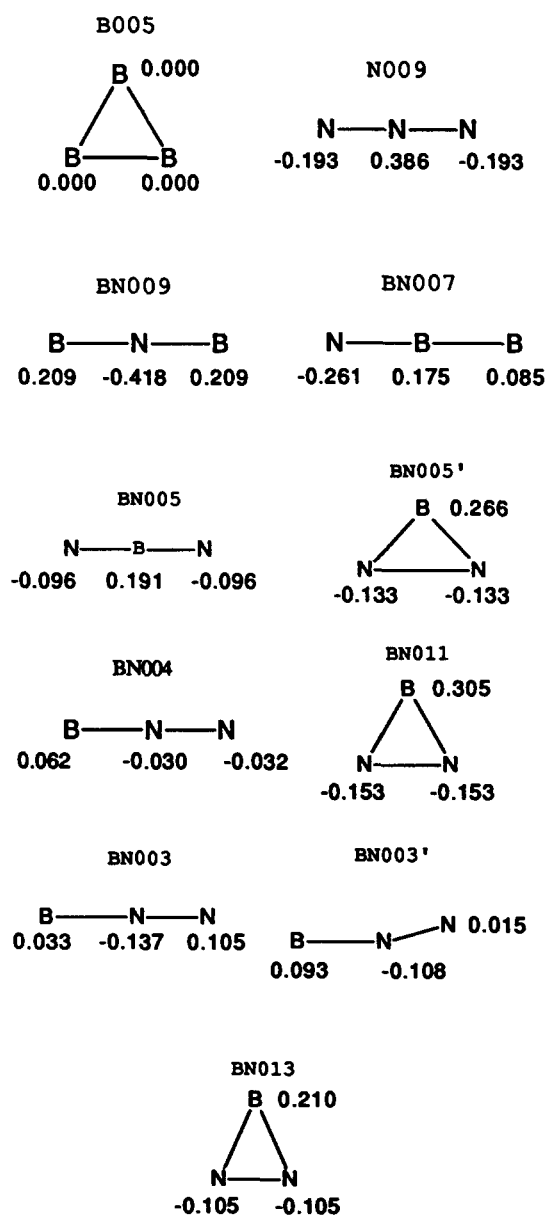
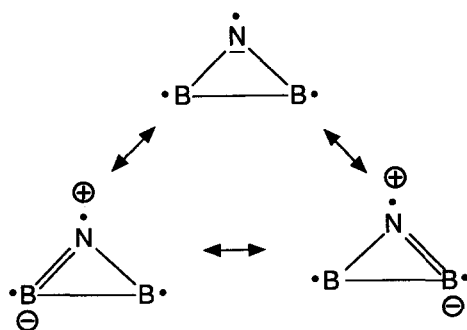


FIG. 5. Mulliken charge distributions (UHF/6-31G*) for the most important clusters.

electrons, but appears to have a quite different electronic structure, as judged from the large B–B distance. Its resonance structures are



A certain analogy with the triplet state of C₃ can again be seen, in that the cyclic structure lies lower than the linear one

(B₂N⁻ is isoelectronic with C₃). In C₃, the ³A₂' state lies 24.4 kcal mol⁻¹ above the ¹Σ_g⁺ ground state at the UMP4/6-31G* level,⁵⁰ whereas the ³Π_u state lies 47.0 kcal mol⁻¹ above the ground state in a MRD-CI/DZ(+ bond functions) treatment,⁵¹ and 48.4 kcal mol⁻¹ experimentally.⁵²

Finally, from the scaled CC procedure, a binding energy of 269.7 kcal mol⁻¹ is predicted; this corresponds to a dissociation energy of 265.0 kcal mol⁻¹.

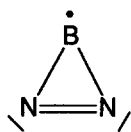
D. BN₂

The situation here is rather complex. At the 3-21G level, convergence failure was even observed for structure BN005. Here, the linear quartet structures BN006 (symmetric) followed by BN004 (asymmetric) are predicted to be most stable. At the DZP level (6-31G*) on the other hand, the order of BN006 and BN004 is reversed and the bent doublet structure BN013 is stabilized. Inclusion of electron correlation lets BN004 and BN013 approach each other in energy. When spin projection is included, the symmetric linear doublet structure BN005 approaches BN004 (again because of larger correlation energy). An asymmetric linear doublet BN003 was only found after considerable numerical difficulty. Even then, a state with a lower Hartree–Fock energy persisted, having a nonzero gradient component on the bond angle. Reoptimization without the linearity constraint led to divergence of the geometry optimization, because of apparent crossing of several states. At the correlated level, BN003 appears to be the most stable structure at this point. With inclusion of spin projection, BN005 is only very little above.

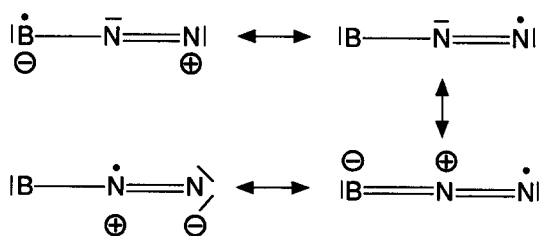
Both BN003 and BN005 are cases of “strong” Renner–Teller effect, in that one of both zero-order Renner–Teller frequencies is imaginary. This corresponds to case (c) in the paper by Lee *et al.*⁵³ Perturbation of the linear geometry leads in the case of BN003 to a slightly bent structure BN003', which was only reached after considerable numerical effort due to oscillation between several states. There is, however, a distinct possibility that the bent structure is an artifact of the theoretical model: a very strong spin contamination should be noted. It should also be remarked that if a lower energy wave function exists at the Hartree–Fock level, the HF frequency calculation may give imaginary frequencies for some modes; this may be the problem with BN003 too. At the MP2 to MP4 levels, the bent structure is less stable than the linear one. At the PMP2 to PMP4 levels, on the other hand, the Hartree–Fock result is confirmed, but the separation is less than 1 kcal mol⁻¹ at the PMP4 level. At both the CCD and CCD + ST(CCD) levels, the linear structure becomes distinctly more stable, by 6.9 and 6.0 kcal mol⁻¹, respectively. Clearly, recalculation of the force constant matrix at a correlated level with a greater basis set would only lead to “weak” Renner–Teller effects. It is noted, that a false angular distortion of linear C₃ was found at the CI level with a (9s5p2d)/[4s2p1d] basis set by Liskow *et al.*⁵⁴ Perturbation of the bond angle in BN005 leads to a ²A₂ state BN005' first, but at a bond angle around 60 deg crossing with an ²A₁ state BN011 is observed, which seems to represent the global minimum. BN005' lies significantly higher than BN005 at any correlated level, so the “strong” Renner–Teller effect might be an artifact of the UHF/

6-31G* force constant matrix. Again, a potential surface study at some correlated level would be very helpful. BN011 is separated only 3.01 kcal mol⁻¹ from BN003, and 3.86 kcal mol⁻¹ from BN005 at the extrapolated PMP level. At the CCD and CCD + ST(CCD) levels, however, the separation from BN005 becomes quite marked (22.8 kcal mol⁻¹); with respect to BN003 the separation remains modest at 4.4 kcal mol⁻¹. At elevated temperatures, this separation does not mean too much: it corresponds to an isomerization constant of merely 1.7 at 4000 K. BN011 is also only 10.71 kcal mol⁻¹ removed from the quartet state BN004, which may thus become more important at higher temperatures because of the additional degeneracy entropy. BN005 will be less important. Therefore, at this stage, the structure of BN₂ in a cluster plasma is best thought of as a mixture of BN011 and BN003 in about equal amounts, with also significant contributions from BN004. This makes three different states in all to be considered for BN₂. A detailed analysis follows in Sec. IV.

On pure energy grounds, BN011 represents the ground state. Based on the Mulliken population analysis and the calculated bond distances, the Lewis structure of BN011 is best thought of as



The corresponding Lewis structures for BN003 and BN004 are resonance hybrids



and



respectively. Judged from these resonance structures, BN003 and BN011 are best thought of as a N₂ molecule with a B atom attached to it, BN003 representing the axial, and BN011 the lateral adduct. This is not the case for BN004, where the calculated B–N and N–N bond distances differ much less, and the N–N distance is markedly higher than that of the N₂ molecule. Note also that BN011 has a rather high degree of charge polarization in the Mulliken population analysis, while this is much less the case for BN003. BN004 has essentially almost equal charges on all atoms, which is readily seen to be in agreement with the resonance hybrids.

BN013 lies relatively low: however, it is found to be a transition state at the UHF/6-31G* level. However, evaluation of the force constant matrix at some correlated level

and/or with a larger basis set may characterize it as a local minimum. It also does not benefit from the additional degeneracy entropy of BN004, so it will be even less important, even at higher temperatures.

For the four lowest-lying states and their UHF/6-31G* Renner–Teller distortions (for the linear cases), harmonic frequencies, IR, and Raman intensities are given in Table VII. BN003 has two ionization potentials that are about equal: 9.95 eV (π , leading to a $^1\Sigma^+$ state), and 9.96 eV (σ , leading to a $^3\Pi$ state). BN003' has its VIP1 at 9.80 eV (a'' , leading to a $^1A''$ state). BN005 has a VIP1 of 11.83 eV (π_u , leading to a $^3\Delta_u$ state). BN011 has its VIP1 at 11.13 eV (b_2 , leading to a 3B_2 state), while the VIP1 of BN004 lies at 10.11 eV (π , leading to a $^3\Pi$ state). Finally, the scaled CC binding energies (dissociation energies between parentheses) are given: BN003 225.3 (221.1) kcal mol⁻¹, BN004 218.1 (213.2) kcal mol⁻¹, BN005 204.1 (200.0) kcal mol⁻¹, BN011 230.4 (224.9) kcal mol⁻¹, and BN013 219.6 (215.9) kcal mol⁻¹.

E. N₃

With the 3-21G basis, most species appear to be unbound (Table II), even the linear doublet N009 corresponding to the experimental ground state. On progressing to the 6-31G* basis set, this problem is partially relieved. The increases in dissociation energy are nevertheless spectacular: on the order of 80 kcal mol⁻¹ for the cyclic structures! This agrees with the statement about polarization functions and ring strain: however, the effect is on a much larger scale here. The phenomenon also appears with the two linear structures, be it to a lesser extent. It is however known, that calculations on N₂ are very sensitive towards expansion of the polarization basis.⁵⁵ When electron correlation is taken into account, the picture changes considerably. The tendency for oscillation of the Møller–Plesset series observed⁵⁶ for N₂ is not seen here. Spin projection has a non-negligible effect on the dissociation energy at the MP2 level, a little less at the MP4 level.

At the highest level of theory considered here, the linear $^2\Pi_g$ state found experimentally is most stable, followed ~ 33 kcal mol⁻¹ higher by the C_{2v} structure N005 with an apical angle of 69.13 deg. The N007 structure with apex angle 49.49 deg is also a local minimum, now at ~ 35 kcal mol⁻¹ above the ground state. Both structures are connected by the Jahn–Teller crossing N003, which should be regarded as the crossing between a 2A_2 state (N005) and a 2B_1 state (N007).

N010 exhibits strong Renner–Teller effect: it deforms to the structure N010', which lies 50 kcal mol⁻¹ or more below N010 at all levels.

All other structures lie much higher. N006 and N008, both C_{2v} , are found as transition states along their B_2 mode: considering the low imaginary frequencies, and the already very high location of both states, the possible C_s local minimum is left out of consideration here. A D_{3h} structure with term $^4A'_1$ is found as a local minimum: it is however so high-lying that it may safely be neglected.

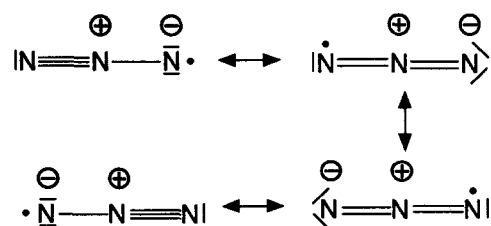
The structures N005 and N007 might eventually play minor roles at very high temperatures (4000 K or more).

The lifetime of these species under such conditions is still open to debate.

N005 was not found in the study by Novaro *et al.*: these authors used the simple split-valence 4-31G basis set, however, and no electron correlation at all. So, any results can only be deceptive for the kind of problem under study, in regard of the high sensitivity to the polarization space. In the present study, plainly absurd geometries were often found at the 3-21G level. In the case of N006, divergence of the geometry optimization was even observed. None of these problems occurred at the 6-31G* level.

At this level, the spectroscopic parameters for N_3 are predicted as: ${}^2\Pi_g$, bond length 1.1593 Å, frequencies 1516 cm^{-1} (Σ_u , 654 km mol^{-1}), 1238 cm^{-1} (Σ_g , IR inactive) and 538 cm^{-1} (Π_u , 18 km mol^{-1}). The latter value is simply the average of the two zero-order Renner–Teller frequencies. All predictions are in reasonable agreement with the experimental result (in a noble gas matrix) of 1.1815 Å, and IR peaks at 1657 cm^{-1} (strong, Σ_u), 2945 cm^{-1} (weak, combination mode Σ_g and Σ_u), and 473 cm^{-1} (weak, Π_u). Analogous results were found by the experimentors with a 6-311G* basis set. A very recent Fourier transform IR study⁵⁷ predicts a value of 1.181 15 Å in the gas phase, and 1644.6784 cm^{-1} for the Σ_u mode. Adamowicz⁵⁸ finds 1.186 Å at the MP4 level, and 1.181 Å at the CCSD level, in either case with a 6-311G* basis set. We further predict a vertical ionization potential of 10.77 eV (π_g , leading to a ${}^3\Sigma_g^-$ state) which is in fair agreement with the experimental value⁵⁹ of 11.06 eV, as well as with the observed⁶⁰ triplet ground state and $D_{\infty h}$ point group for N_3^+ .

Note that all canonical structures for N009



have a positive formal charge on the central nitrogen atom: this explains the very high degree of charge polarization found in the Mulliken population analysis (Fig. 5).

Finally, the scaled CC method predicts a binding energy of 215.7 kcal mol^{-1} , or a dissociation energy of 210.1 kcal mol^{-1} . Experimentally, the heat of formation at absolute zero of N_3 is given⁶¹ as $468 \pm 21 \text{ kJ mol}^{-1}$ or $111.9 \pm 5.0 \text{ kcal mol}^{-1}$. Combined with the heat of formation at absolute zero of the N atom⁶² (112.534 kcal mol^{-1}), this yields a dissociation energy of $225.7 \pm 5 \text{ kcal mol}^{-1}$. Older references⁶³ give a value of $99.7 \pm 5 \text{ kcal mol}^{-1}$ for the heat of formation, resulting in a dissociation energy of $237.9 \pm 5 \text{ kcal mol}^{-1}$. The discrepancy between theoretical and experimental values is somewhat overly large: errors in the experimental values cannot be ruled out.

IV. SOME THERMOCHEMICAL CONSIDERATIONS

Seifert *et al.*¹⁸ made some thermochemical considerations about the possible fragmentation schemes for the boron–nitrogen clusters. They, however, did not investigate the temperature dependence of the equilibria. For B_2N , basically three different fragmentation schemes are possible (they only considered linear structures):

TABLE V. Molecular energies (hartree) and binding energies (kcal mol^{-1}) of the clusters at the CCD/6-31G* and CCD + ST(CCD)/631G* levels, as well as scaled CCD + ST(CCD)/6-31G* binding energies.

Species	Molecular energy			Binding energy			
	E(UHF)	E(CCD)	E(CCD + ST)	UHF	CCD	CCD + ST	Scaled ^a
$B({}^2P)$	-24.522 04	-24.578 35	-24.579 62				
$N({}^4S)$	-54.385 44	-54.472 91	-54.473 75				
$B_2({}^3\Sigma_g^-)$	-49.076 87	-49.240 63	-49.260 03	20.58	52.67	63.25	72.74
$B_2({}^5\Sigma_u^-)$	-49.157 84	-49.251 81	-49.256 70	71.39	59.68	61.16	70.33
$BN({}^3\Pi)$	-78.990 16	-79.183 14	-79.194 53	51.88	82.76	88.58	101.87
$BN({}^1\Sigma^+)$	-78.882 62	-79.152 90	-79.187 76	-15.60	63.78	84.33	96.98
N_2	-108.943 95	-109.249 25	-109.264 12	108.60	190.40	198.68	228.48
B005	-73.772 07	-73.990 26	-74.018 73	129.24	160.15	175.62	201.96
BN007	-103.649 80	-103.885 66	-103.903 22	138.23	160.67	169.57	195.01
BN009	-103.673 88	-103.979 74	-104.006 72	153.34	219.71	234.52	269.70
BN003	-133.448 99	-133.818 23	-133.839 30	97.93	184.53	195.90	225.29
BN003'	-133.455 91	-133.807 30	-133.829 80	102.28	177.67	189.93	218.42
BN004	-133.484 55	-133.809 64	-133.829 30	120.25	179.14	189.62	218.06
BN005	-133.375 73	-133.765 07	-133.810 01	51.96	151.17	177.52	204.15
BN005'	-133.393 43	-133.747 82	-133.778 73	63.07	140.35	157.89	181.57
BN011	-133.459 13	-133.826 64	-133.846 36	104.30	189.81	200.33	230.38
BN013	-133.430 89	-133.810 37	-133.831 39	86.58	179.60	190.94	219.58
N009	-163.245 78	-163.691 41	-163.720 17	56.14	171.11	187.58	215.72

^a CCD + ST(CCD)/6-31G* binding energies scaled by 1.15 (see the text).

TABLE VI. Reaction energies (kcal mol⁻¹) at the UMP4,PMP4,CCD, and CCD + ST (CCD) levels (this work), and with the local density approximation (Ref. 18).

Reaction	MP4	PMP4	MP _{xtrp.}	PMP _{xtrp.}	CCD	CCD + ST	scaled ^a	LDA ^b
B ₃ →B ₂ + B	4.86	5.46	4.82	5.41	2.51	4.87	5.60	...
N ₃ →N ₂ + N	-0.42	-0.20	-0.39	-0.18	-2.27	-0.48	-0.55	...
B ₂ N→BN + B	6.53	6.51	6.53	6.51	4.40	6.33	7.28	9.3
B ₂ N→B ₂ + N	7.56	7.58	7.51	7.52	3.55	7.43	8.54	17.7
BN ₂ →BN + N	4.95	4.91	4.94	4.91	2.27	4.85	5.58	10.9
BN ₂ →N ₂ + B	0.14	0.15	0.08	0.09	-0.19	0.07	0.08	1.5

^a From CCD + ST(CCD) binding energies scaled by 1.15 (see the text).

^b Reference 18.

- (a) BBN→B₂ + N
- (b) BBN→B + BN
- (c) BNB→BN + B.

For BN₂, the following three fragmentation reactions were considered:

- (a) BNN→B + N₂
- (b) BNN→BN + N
- (c) NBN→BN + N.

They concluded from their calculations that BNN will be more stable than NBN, and that BNN readily decays to N₂ and B. On the other hand, BNB will be more stable than NBB, and does not decay spontaneously. This is in agreement with the fact, that B₂N is observed in mass spectra, while BN₂ is not.

Table VI lists the reaction energies obtained at the MP4/6-31G*, PMP4/6-31G*, CCD/6-31G*, and CCD + ST(CCD)/6-31G* levels, along with the LCAO-LDA values from Ref. 18. It is immediately seen, that although the different *ab initio* theories all give values within the same range, the LCAO-LDA reaction energies are greatly exaggerated. It is also evident from these results that the triples contribution is very important.

Comparing the qualitative conclusions of Seifert *et al.* with ours, it is confirmed that BNB (our structure BN009) is more stable than BBN (our structure BN007), and that BNB will not dissociate spontaneously in either BN + B or B₂ + N. We also find confirmation for their conclusion that BNN is more stable than NBN, but find a cyclic structure (not considered by them) to be the global minimum.

To investigate the effect of temperature on the equilibrium constants of the various reactions involved, partition functions were set up using moments of inertia from the UHF/6-31G* structures, and harmonic frequencies scaled by 0.89. The formulas concerned are discussed in every textbook on statistical thermodynamics⁶⁴; convenient numerical expressions may also be found in Herzberg,⁶⁵ although the most recent values for the fundamental constants⁶⁶ were used in the present work. The individual contributions of the isomers and/or states were then weighed⁶⁷ to obtain the global thermodynamic quantities.

Several possible errors may arise in these calculations. The first one is the error in the computed binding energies. Since we are primarily interested in the high temperature behavior, the expected magnitude of errors will not change

any conclusions significantly. The second one is the error in the computed frequencies. Here, the use of a common scaling factor based on a very large sample of IR frequencies will generally result in error cancellation (note the excellent agreement between calculated and experimental zero-point energies for N₃), whereas the small magnitude of the zero-point corrections will make any remaining errors completely negligible. The third one is the use of HF/31G* geometries and frequencies for the calculation of reaction entropies. As pointed out in a study by Hout *et al.*,⁶⁸ computed HF/6-31G* absolute and reaction entropies are in good agreement with experiment at room temperature. The discrepancies might become larger at higher temperatures, but will then be linked to the fourth possible source of error: the RHHO (rigid rotator-harmonic oscillator) approximation.⁶⁹ For a variety of reactions and molecules, it was shown not to present any problem⁷⁰ up to even 2000 K. For the species with low bending vibrations however, such as B₂N, the same problems will occur for the entropy as for C₃, where anharmonicity and vibration–rotation coupling had to be taken into account to obtain satisfactory agreement between the experimental second- and third-law entropies.⁷¹ The difference, on the order of 4 e.u. for C₃, might have significant consequences for the equilibrium constants at high temperatures. The solution is not trivial. To predict harmonic bending frequencies for multiple bonded molecules accurately, MP2 force constants with a basis set of at least TZ(2df) quality seem prerequisite.⁷² For the anharmonic corrections, cubic and quartic HF/DZP force constants can be used together with formulas derived from perturbation theory.⁷³ Since correlated frequencies would also remedy the qualitative misbehavior in the UHF/6-31G* force fields in some instances, the authors plan to perform such an analysis in the near future.

The fifth potential error source has to do with the relative energies of the different states. Judged from the CCD + ST(CCD) results for B₂ and BN, the sequence of states is probably reliable, but improved values for the state splittings might also affect the partition functions. To this end, calculations with greater basis sets also seem appropriate. This might also achieve a lesser dependency on scaling procedures for the binding energies: combined bond-polarization function basis sets⁷⁴ are possible candidates. For the isomeric composition at higher temperatures, however, the problem is also strongly related to the previous one.

Finally, the proper isotopic composition of B has not

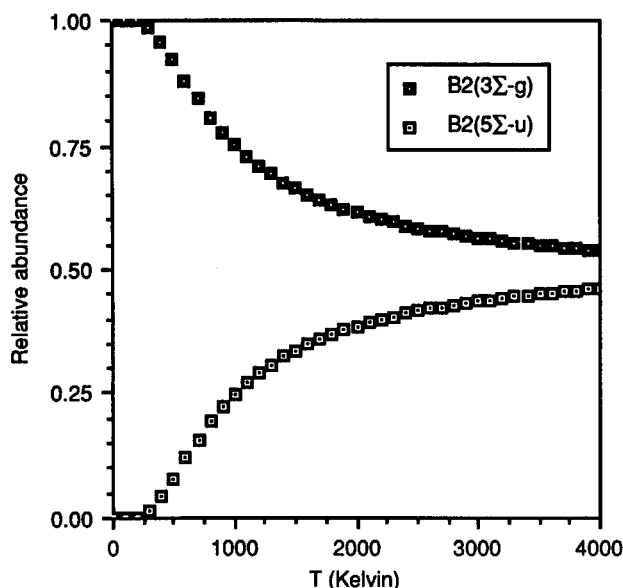


FIG. 6. Relative abundances of the ${}^3\Sigma_g^-$ and ${}^5\Sigma_u^-$ states of B_2 as a function of temperature.

been accounted for. The most abundant isotope used throughout in this work, ${}^{11}\text{B}$, has an abundance of 80.22%; the other naturally occurring isotope ${}^{10}\text{B}$ makes up 19.78% of the total. For species composed entirely of the lighter isotope, vibrational frequencies would be higher by a factor $(11/10)^{1/2}$, or 1.05. Translational entropies would be lowered somewhat for these species. For the global entropy, the errors incurred will however be negligible against the other errors inherent in this treatment. The error in the case of nitrogen, with a ${}^{14}\text{N}$ abundance of 99.63%, is of course negligible whatsoever.

Figure 6 presents the relative abundances of the ${}^3\Sigma_g^-$ and ${}^5\Sigma_u^-$ states of B_2 as a function of temperature. It is clearly seen, how unimportant the small excitation energy be-

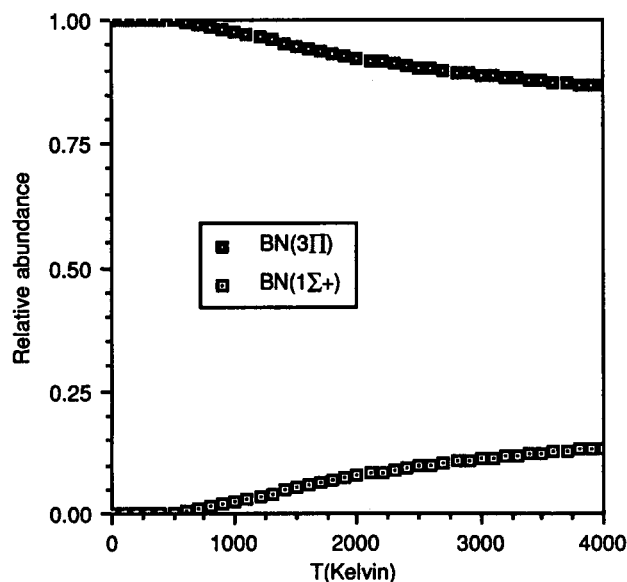


FIG. 7. Relative abundances of the ${}^3\Pi$ and ${}^1\Sigma^+$ states of BN as a function of temperature.

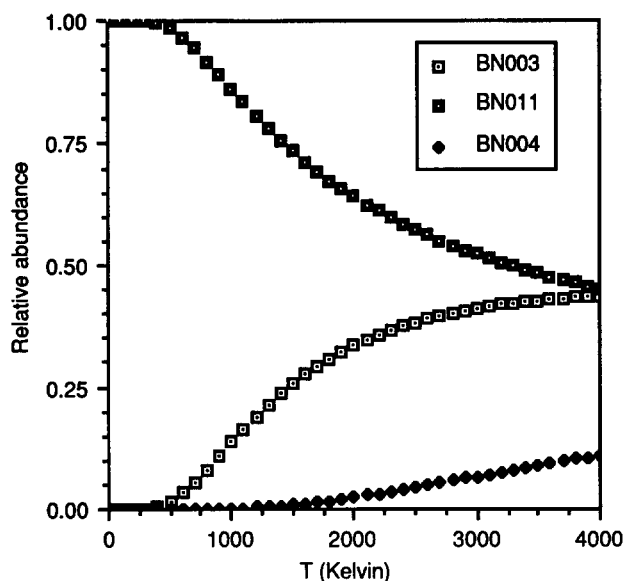


FIG. 8. Relative abundances of the 2A_1 (BN011), ${}^2\Pi$ (BN003), and ${}^4\Sigma^-$ (BN004) states of BN_2 as a function of temperature.

comes at elevated temperatures. Figure 7 presents the same for the ${}^1\Sigma^+$ and ${}^3\Pi$ states of BN . Here, the triplet state benefits from its additional degeneracy entropy, and still makes up 85% of the total even at 4000 K. Figure 8 then, presents the relative abundances of structures BN003, BN004, and BN011 in BN_2 . (The false Renner–Teller distortion in BN003 presented a problem here; therefore, it was decided to use the BN003 binding energy, but to set up the partition functions using data from BN003'.) Here, BN011 outweighs the others at lower temperatures, but might become slightly surpassed by BN003 at higher temperatures, where BN004 can play a role too because of its additional degeneracy entropy. The relative behavior of BN003 and BN011 might however be shifted in favor of the latter when the anharmonic behavior of the low bending frequencies of BN003 (replaced here by the low bending frequency of BN003') were properly accounted for in the entropy.

Table VIII presents values for the association enthalpy, entropy, and free energy from the partition functions, as well as values for the absolute entropy. Figures 9 to 12 present plots of $\log K$ against reciprocal temperature for all dissociation reactions of the B_3 , $B_2\text{N}$, BN_2 , and N_3 systems, respectively. Note the high degree of linearity in all curves.

B_3 is clearly stable against decay to B_2 and B at all temperatures except the very highest, and against atomization up to about 3100 K. So it may be expected to be present at lower plasma temperatures. It is found⁷⁵ in double-focused mass spectra from a laser plasma.⁷⁶ $B_2\text{N}$ will only atomize above 4000 K. It is distinctly stable against decay to BN and B , as well as to B_2 and N . It is indeed found in laser mass spectra of solid boron nitride, and in high abundance.⁷⁵ BN_2 is stable against atomization up to about 3300 K, but the dissociation to B and N_2 proceeds completely at all temperatures. This explains the absence of BN_2 in the mass spectra mentioned above. It is however stable towards dissociation to BN and N up to about 3600 K. N_3 is stable against atomization up to about 2850 K: if our calculated dissociation

TABLE VII. Harmonic frequencies (scaled by 0.89) and corresponding zero-point energies, IR intensities (km mol^{-1}) and Raman activities ($\text{\AA}^4/\text{a.m.u.}$) of the most important clusters.

Struc- ture	For- mula	Point group	Term	ν_4			ν_3			ν_2			ν_1			E_{zp} (kcal mol $^{-1}$)
				(cm $^{-1}$)	(IR)	Raman)	(cm $^{-1}$)	(IR)	Raman)	(cm $^{-1}$)	(IR)	Raman)	(cm $^{-1}$)	(IR)	Raman)	
B ₂	B ₂	$D_{\infty h}$	$^3\Sigma_g^-$									967	(0 99)	Σ_g	1.38	
B ₂	B ₂	$D_{\infty h}$	$^5\Sigma_u^-$									1242	(0 180)	Σ_g	1.78	
BN	BN	$C_{\infty v}$	$^3\Pi$									1572	(27 80)	Σ	2.25	
BN	BN	$C_{\infty v}$	$^1\Sigma^+$									1682	(75 inf)	Σ	2.40	
N ₂	N ₂	$D_{\infty h}$	$^+\Sigma_g^+$									2455	(0 18)	Σ_g	3.51	
B005	B ₃	D_{3h}	$^2A_1'$				865	(32 0.4)	E'	865	(32 0.4)	E'	1084	(0 43)	A_1'	4.02
BN007	B ₂ N	$C_{\infty v}$	$^2\Sigma^+$	269	(9 22)	Π	269	(9 22)	Π	825	(4 36)	Σ	1438	(160 536)	Σ	4.01
BN009	B ₂ N	$D_{\infty h}$	$^2\Sigma_u^+$	73	(5 0)	Π_u	73	(5 0)	Π_u	1108	(0 24)	Σ_g	2021	(8782 0)	Σ_u	4.68
BN003	BN ₂	$C_{\infty v}$	$^2\Pi$	101 <i>i</i>	(13 141)	Π	255	(21 7)	Π	904	(147 134)	Σ	1783	(3 250)	Σ	4.20
BN003'	BN ₂	C_s	$^2A''$				271	(20 533)	A''	935	(51 78)	A'	1622	(68 45)	A'	4.04
BN004	BN ₂	C_v	$^4\Sigma^-$	410	(0.4 4)	Π	410	(0.4 4)	Π	1160	(16 19)	Σ	1441	(196 136)	Σ	4.89
BN005	BN ₂	$D_{\infty h}$	$^2\Pi_g$	841 <i>i</i>	(128 0)	Π_u	188	(19 0)	Π_u	1003	(0 inf) ^a	Σ_g	1696	(1225 16)	Σ_u	4.13
BN005'	BN ₂	C_{2v}	2A_1				1035 <i>i</i>	(1695 49 471)	B_2	355	(31 inf)	A_1	1224	(58 41 938)	A_1	2.26
BN011	BN ₂	C_{2v}	2A_1				1087	(1 4)	B_2	1148	(27 14)	A_1	1566	(26 28)	A_1	5.43
BN013	BN ₂	C_{2v}	2B_2				223 <i>i</i>	(11 0.3)	B_2	652	(186 109)	A_1	1919	(34 104)	A_1	3.68
N009	N ₃	$D_{\infty h}$	$^2\Pi_g$	472	(18 0)	Π_u	605	(15 0)	Π_u	1238	(0 186)	Σ_g	1516	(654 0)	Σ_u	5.62

^ainf signifies numerical overflow (100 000 or more).

energy is indeed an underestimate, this temperature will shift even higher. However, due to the extraordinary stability of the N₂ molecule, the dissociation in N₂ and N proceeds completely at all temperatures concerned. This explains, why N₃ is not found in the mass spectra either.

V. CONCLUSIONS

The potential surfaces of B₃, B₂N, BN₂, and N₃ have been studied using the 6-31G* basis sets and UHF, MP4, PMP4, CCD, and CCD + ST(CCD) methods. Spin conta-

TABLE VIII. Calculated thermodynamic properties at some selected temperatures.

Temp. (K)	B ₂	BN	N ₂	B ₃	B ₂ N	BN ₂	N ₃
Association enthalpy (kcal mol $^{-1}$)							
0	-71.36	-99.62	-224.98	-197.94	-265.02	-224.94	-210.09
300	-72.19	-100.51	-225.87	-199.93	-266.39	-226.99	-211.02
1000	-72.78	-101.96	-227.75	-202.07	-268.06	-229.12	-210.23
2000	-73.60	-103.06	-229.49	-203.50	-268.81	-229.56	-206.98
3000	-74.53	-104.02	-230.79	-204.64	-269.10	-229.76	-203.26
4000	-75.50	-104.97	-231.95	-205.71	-269.25	-229.96	-199.42
Association entropy (e.u.)							
0	-0.57	-1.95	-5.51	-2.76	-4.13	-5.51	-6.89
300	-29.84	-31.02	-36.82	-60.60	-60.52	-65.00	-71.24
1000	-30.99	-33.72	-40.14	-64.72	-63.68	-69.34	-75.16
2000	-31.55	-34.49	-41.37	-65.74	-64.24	-69.67	-75.69
3000	-31.93	-34.88	-41.91	-66.20	-64.36	-69.75	-75.80
4000	-32.21	-35.16	-42.24	-66.51	-64.40	-69.81	-75.84
Free energy of association (kcal mol $^{-1}$)							
0	-71.36	-71.36	-224.98	-197.94	-265.02	-224.94	-210.09
300	-63.24	-91.20	-214.83	-181.75	-248.23	-207.49	-190.84
1000	-41.79	-68.24	-187.61	-137.35	-204.37	-159.78	-139.05
2000	-10.50	-34.07	-146.74	-72.03	-140.33	-90.22	-63.54
3000	21.26	0.63	-105.08	-6.04	-76.01	-20.50	12.21
4000	53.33	35.65	-62.99	60.32	-11.63	49.28	88.03
Absolute entropy (e.u.)							
0	2.18	2.18	0.00	1.38	1.38	1.38	1.38
300	48.52	49.43	45.73	56.94	59.11	56.73	52.58
1000	59.33	58.70	54.37	70.76	73.89	70.33	66.61
2000	65.66	64.81	60.02	80.08	83.66	80.33	76.40
3000	69.31	68.45	63.52	85.65	89.59	86.29	82.34
4000	71.89	71.03	66.04	89.63	93.83	90.52	86.59

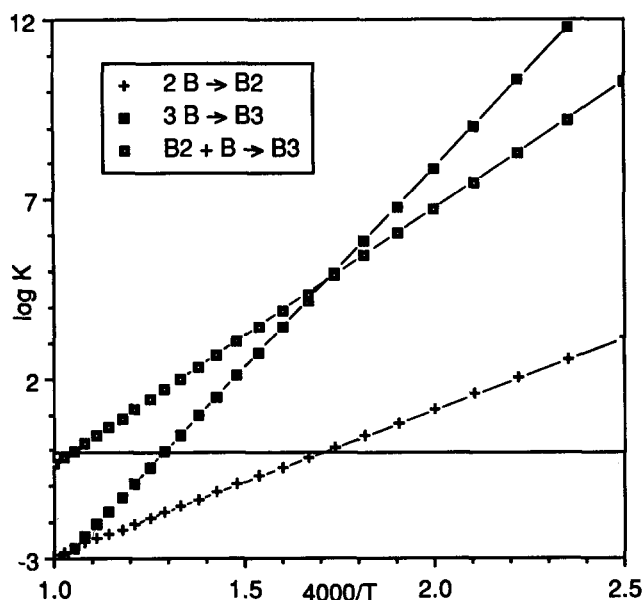


FIG. 9. Plot of $\log K$ vs $4000/T$ for the reactions $2B \rightarrow B_2$, $3B \rightarrow B_3$, and $B_2 + B \rightarrow B_3$.

mination is shown to present severe problems with the MP4 procedure, which are for the most part remedied by the PMP4 procedure. Vibrational frequencies and intensities for all the different stationary points found have been given. The description of the potential surface is shown to be not entirely adequate at the UHF level, even not qualitatively.

B_3 is unambiguously predicted to be an equilateral triangle in its ${}^2A'_1$ ground state. B_2N is found to have a symmetric linear structure and a ${}^2\Sigma_u^+$ ground state, with the asymmetric linear structure possibly being present in small amounts at higher temperatures. The Σ_u mode of the ground state is predicted to be extremely intense. The ground state of BN_2 is found to be an isosceles triangle in a 2A_1 ground state, but ${}^2\Pi$ and ${}^4\Sigma^-$ asymmetric linear structures are close contenders,

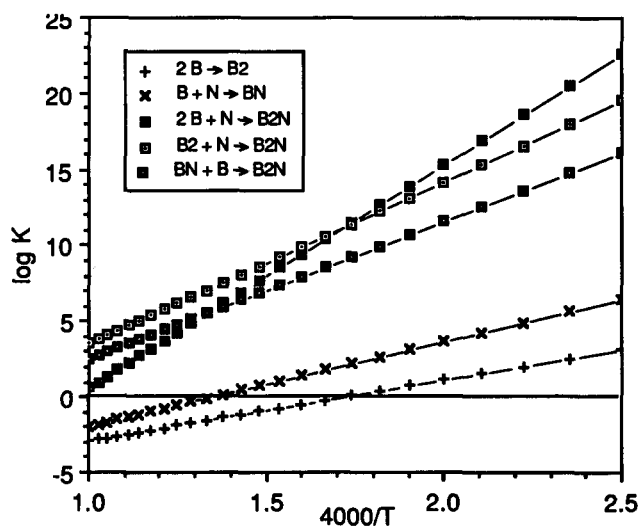


FIG. 10. Plot of $\log K$ vs $4000/T$ for the reactions $2B \rightarrow B_2$, $B + N \rightarrow BN$, $2B + N \rightarrow B_2N$, $B_2 + N \rightarrow B_2N$, and $BN + B \rightarrow B_2N$.

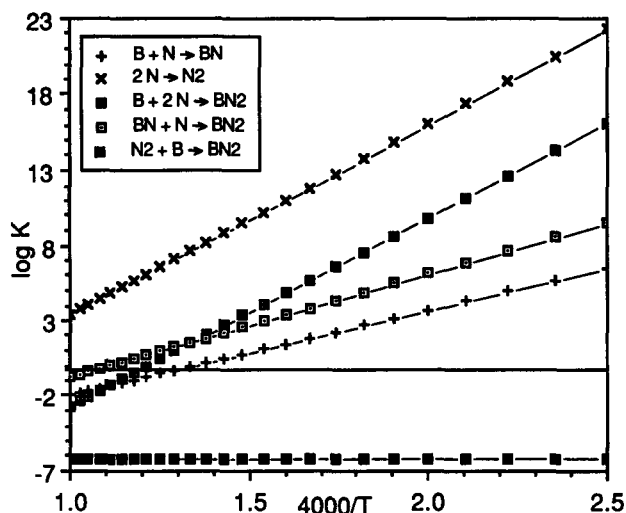


FIG. 11. Plot of $\log K$ vs $4000/T$ for the reactions $B + N \rightarrow BN$, $2N \rightarrow N_2$, $B + 2N \rightarrow BN_2$, $BN + N \rightarrow BN_2$, and $N_2 + B \rightarrow BN_2$.

in that order. The predicted spectroscopic parameters for N_3 agree well with experiment.

For the lowest-lying states, dissociation energies (with an uncertainty on the order of 4 kcal mol^{-1}) are estimated using scaled $CCD + ST(CCD)/6-31G^*$ binding energies. Their predicted values are: BN 99.6, B_3 197.9, B_2N 265.0, BN_2 224.9, and N_3 210.1 kcal mol^{-1} . For N_3 , a discrepancy exists with the approximate experimental data in literature; it cannot be ruled out that these are in error.

Using these estimated dissociation energies, the UHF/6-31G* structural parameters, and the harmonic frequencies, partition functions have been set up within the RRHO approximation. Plots of $\log K$ vs temperature for the dissociation and fragmentation reactions of the clusters are given over the 1600–4000 K range. Absolute and reaction entropies, as well as reaction enthalpies and free energies are given at selected temperatures.

The absence of N_3 and BN_2 , as well as the presence of

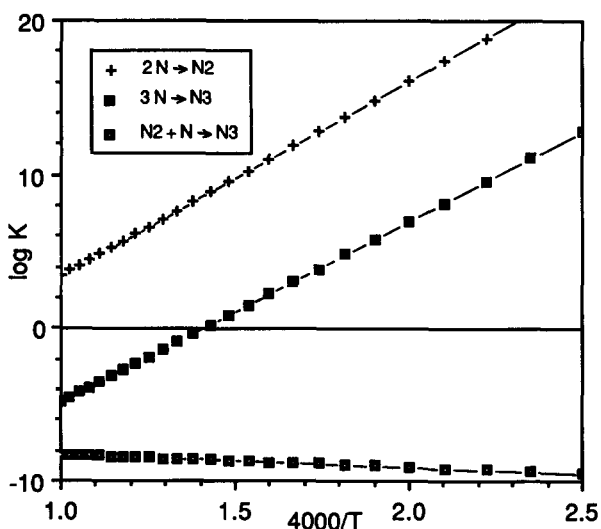


FIG. 12. Plot of $\log K$ vs $4000/T$ for the reactions $2N \rightarrow N_2$, $3N \rightarrow N_3$, and $N_2 + N \rightarrow N_3$.

B_2N and B_3 , in the mass spectra, are explained from a fragmentation analysis. The abundance of B_2N^+ can be explained from the surprisingly low VIP1 of B_2N , as well as its stability.

ACKNOWLEDGMENTS

J. M. L. Martin is indebted to the Belgian National Fund for Scientific Research (NFWO/FNRS) for a contract as research assistant. The authors are also grateful to the Belgian Department of Scientific Policy for a research grant permitting the purchase of the MicroVAX 2000 workstation. This publication forms a part of research results of a program in InterUniversity Attraction Poles, initiated by the Belgian State—Prime Ministers Office—Science Policy Programming.

- ¹*Gmelins Handbook of Inorganic Chemistry*, 8th ed., Boron compounds, 3rd supplement, Vol. 3 (Springer, Berlin, 1988).
- ²T. Takagi, *Vacuum* **36**, 27 (1986).
- ³B. Rother and C. Weissmantel, *Phys. Status Solidi A* **87**, K119 (1985).
- ⁴M. D. Wiggins, C. R. Aita, and F. S. Hickernell, *J. Vac. Sci. Technol. A* **2**, 322 (1984).
- ⁵M. Sokolowski, *J. Cryst. Growth* **46**, 136 (1979).
- ⁶J. Szmidt, A. Jakubowski, A. Michalski, and A. Rusek, *Thin Solid Films* **110**, 7 (1983).
- ⁷M. Satou and F. Fujimoto, *Jpn. J. Appl. Phys.* **22**, L171 (1983).
- ⁸G. Kessler, H.-D. Bauer, W. Pompe, and H. J. Scheibe, *Thin Solid Films* **147**, L45 (1987).
- ⁹ZFI Mitteilungen, nr. 134: Beiträge zur Clusterforschung, Akademie der Wissenschaften der DDR, September 1987.
- ¹⁰W. G. Richards, T. E. H. Walker, and R. K. Hinkley, *A Bibliography of Ab Initio Molecular Wave Functions* (Oxford University, Oxford, 1971); Supplement for 1970–1973 (1974); Supplement for 1974–1977 (1978); supplement for 1978–1980 (1981); K. Ohno and K. Morokuma, *Quantum Chemistry Literature Data Base—Bibliography of ab initio calculations for 1978–1980* (Elsevier, Amsterdam, 1982); Supplement for 1981, *J. Mol. Struct.* **91**, (THEOCHEM 8), 1 (1982); Supplement for 1982, *ibid.* **106** (THEOCHEM 15), 1 (1983); Supplement for 1983, *ibid.* **119** (THEOCHEM 20), 1 (1984); Supplement for 1984, *ibid.* **134** (THEOCHEM 27), 1 (1985); Supplement for 1985, *ibid.* **148** (THEOCHEM 33), 181 (1986); Supplement for 1986, *ibid.* **154** (THEOCHEM 39), 1 (1987).
- ¹¹K. P. Huber and G. Herzberg, *Constants of Diatomic Molecules* (Van Nostrand Reinhold, New York, 1979).
- ¹²K. Raghavachari and J. S. Binkley, *J. Chem. Phys.* **87**, 2191 (1987).
- ¹³M. Dupuis, B. Liu, *J. Chem. Phys.* **68**, 2902 (1978); K. Raghavachari, *ibid.* **82**, 4607 (1985).
- ¹⁴S. P. Karna and F. Grein, *Chem. Phys.* **98**, 207 (1985).
- ¹⁵J. N. Murrell, O. Novaro, and S. Castillo, *Chem. Phys. Letts.* **90**, 421 (1982); O. Novaro, and S. Castillo, *Int. J. Quantum Chem. Symp.* **26**, 41 (1984).
- ¹⁶J. Baker, R. H. Nobes, and L. Radom, *J. Comp. Chem.* **7**, 349 (1986).
- ¹⁷R. Tian, J. C. Facelli, and J. Michl, *J. Phys. Chem.* **92**, 4073 (1988).
- ¹⁸G. Seifert, B. Schwab, S. Becker, and H. J. Dietze, *Int. J. Mass Spectr. Ion Proc.* **85**, 327 (1988).
- ¹⁹W. Bieger, G. Seifert, H. Eschrig, and G. Grossmann, *Z. Phys. Chem. (Leipzig)* **266**, 751 (1985); G. Seifert, H. Eschrig, and W. Bieger, *ibid.* **267**, 529 (1986).
- ²⁰J. S. Binkley, M. J. Frisch, K. Raghavachari, D. J. DeFrees, H. B. Schlegel, R. A. Whiteside, E. M. Fluder, R. Seeger, D. J. Fox, M. Head-Gordon, and S. Topiol, GAUSSIAN 86 release C, Carnegie–Mellon University, Pittsburgh, PA, 1987.
- ²¹J. A. Pople and R. K. Nesbet, *J. Chem. Phys.* **22**, 571 (1954).
- ²²M. J. S. Dewar and W. Thiel, *J. Am. Chem. Soc.* **99**, 4899 (1977); *Theor. Chim. Acta* **46**, 89 (1977).
- ²³J. S. Binkley, J. A. Pople, and W. J. Hehre, *J. Am. Chem. Soc.* **102**, 939 (1980).
- ²⁴H. B. Schlegel, *J. Comp. Chem.* **3**, 214 (1982).
- ²⁵H. B. Schlegel, *Theor. Chim. Acta* **66**, 333 (1984).
- ²⁶W. J. Hehre, R. Ditchfield, and J. A. Pople, *J. Chem. Phys.* **56**, 2257 (1972); P. C. Hariharan and J. A. Pople, *Chem. Phys. Lett.* **16**, 217 (1972); *Theor. Chim. Acta* **28**, 213 (1973).
- ²⁷J. A. Pople, R. Krishnan, H. B. Schlegel, and J. S. Binkley, *Int. J. Quantum Chem. Symp.* **13**, 225 (1979).
- ²⁸B. A. Hess, Jr., L. J. Schaad, P. Carsky, and R. Z. Zahradnik, *Chem. Rev.* **86**, 709 (1986).
- ²⁹C. Möller and M. S. Plesset, *Phys. Rev.* **46**, 618 (1934); J. S. Binkley and J. A. Pople, *Int. J. Quantum Chem.* **9**, 229 (1975); J. A. Pople, J. S. Binkley, and R. Seeger, *Int. J. Quantum Chem. Symp.* **10**, 1 (1976); R. Krishnan and J. A. Pople, *Int. J. Quantum Chem.* **14**, 91 (1978); R. Krishnan, M. J. Frisch, and J. A. Pople, *J. Chem. Phys.* **72**, 4244 (1980).
- ³⁰H. B. Schlegel, *J. Chem. Phys.* **84**, 4530 (1986).
- ³¹J. A. Pople, M. J. Frisch, B. T. Luke, and J. S. Binkley, *Int. J. Quantum Chem. Symp.* **17**, 307 (1983).
- ³²R. Seeger and J. A. Pople, *J. Chem. Phys.* **66**, 3045 (1977).
- ³³R. Seeger and J. A. Pople, *J. Chem. Phys.* **65**, 265 (1976).
- ³⁴L. A. Farnell, J. A. Pople, and L. Radom, *J. Phys. Chem.* **87**, 79 (1983).
- ³⁵N. C. Handy, P. J. Knowles, and K. Somasundram, *Theor. Chim. Acta* **68**, 87 (1985).
- ³⁶K. Raghavachari, *J. Chem. Phys.* **82**, 4607 (1985).
- ³⁷H. B. Schlegel, *J. Phys. Chem.* **92**, 3075 (1988).
- ³⁸R. S. Mulliken, *J. Chem. Phys.* **23**, 1833, 1841, 2338, 2343 (1955).
- ³⁹T. Koopmans, *Physica* **1**, 69 (1934).
- ⁴⁰M. E. Schwartz, in *Modern Quantum Chemistry*, edited by H. F. Schaefer III (Plenum, New York, 1977), Vol. 4, o. 357.
- ⁴¹M. J. Frisch, J. A. Pople, and J. S. Binkley, *J. Chem. Phys.* **80**, 3265 (1984).
- ⁴²K. Raghavachari, *J. Chem. Phys.* **84**, 5672 (1986).
- ⁴³A. G. Gaydon, *Dissociation Energies*, 2nd ed. (Chapman and Hall, London, 1953).
- ⁴⁴*JANAF Thermochemical Tables*, 2nd ed., edited by D. R. Stull and H. R. Prophet, NSRDS-NBS 37 (National Bureau of Standards, Washington, DC, 1971).
- ⁴⁵P. C. Hariharan and J. A. Pople, *Chem. Phys. Lett.* **16**, 217 (1972); see also R. A. Whiteside, R. Krishnan, M. J. Frisch, J. A. Pople, and P. von Ragué Schleyer, *ibid.* **80**, 547 (1981), for the effect on C_3 .
- ⁴⁶J. A. Pople, H. B. Schlegel, R. Krishnan, D. J. DeFrees, J. S. Binkley, M. J. Frisch, R. A. Whiteside, R. F. Hout, and W. J. Hehre, *Int. J. Quantum Chem. Symp.* **15**, 269 (1981).
- ⁴⁷D. H. Liskow, C. F. Bender, and H. F. Schaefer III, *J. Chem. Phys.* **56**, 5075 (1972).
- ⁴⁸L. Gausset, G. Herzberg, A. Lagerqvist, and A. Rosen, *Discuss. Faraday Soc.* **35**, 113 (1963); *Astrophys. J.* **45**, 142 (1965).
- ⁴⁹B. Roos, in *Computational Methods in Quantum Chemistry and Molecular Physics*, edited by G. H. F. Diercksen, B. T. Sutcliffe, and A. Veillard (Reidel, Boston, 1977), Vol. 15, p. 251.
- ⁵⁰R. A. Whiteside, R. Krishnan, M. J. Frisch, J. A. Pople, and P. von Ragué Schleyer, *Chem. Phys. Lett.* **80**, 547 (1981).
- ⁵¹J. Peric-Radic, J. Römelt, S. D. Peyerimhoff, and R. J. Buenker, *Chem. Phys. Lett.* **50**, 344 (1977).
- ⁵²W. Weltner, Jr., and D. McLeod, Jr., *J. Chem. Phys.* **45**, 3096 (1966); **40**, 1305 (1964).
- ⁵³T. J. Lee, D. J. Fox, H. F. Schaefer III, and R. M. Pitzer, *J. Chem. Phys.* **81**, 356 (1984).
- ⁵⁴D. H. Liskow, C. F. Bender, and H. F. Schaefer III, *J. Chem. Phys.* **56**, 5075 (1972).
- ⁵⁵J. S. Binkley and M. J. Frisch, *Int. J. Quantum Chem. Symp.* **17**, 337 (1983).
- ⁵⁶M. J. Frisch, J. S. Binkley, and J. A. Pople, *J. Chem. Phys.* **80**, 3268 (1984).
- ⁵⁷C. R. Baizer, P. F. Bernath, J. B. Burkholder, and C. J. Howard, *J. Chem. Phys.* **89**, 1762 (1988).
- ⁵⁸L. Adamowicz (personal communication quoted in previous reference).
- ⁵⁹J. M. Dyke, N. B. H. Jonathan, A. E. Lewis, and A. Morris, *Mol. Phys.* **47**, 1231 (1982).
- ⁶⁰A. E. Douglas, and W. J. Jones, *Can. J. Phys.* **43**, 2116 (1965); M. Polak, M. Gruebele, and R. J. Saykally, *J. Am. Chem. Soc.* **109**, 2884 (1987).
- ⁶¹M. J. Pellerite, R. L. Jackson, J. I. Braumann, *J. Phys. Chem.* **85**, 1624 (1981).
- ⁶²*Handbook of Chemistry and Physics*, 64th ed. (CRC, Boca Raton, Florida, 1984).
- ⁶³M. W. Chase, J. L. Curnutt, A. T. Hu, H. Prophet, A. N. Syverud, and L. C. Walker, *J. Phys. Chem. Ref. Data* **4**, 1 (1975); T. C. Clark and M. A. A. Clyne, *Trans. Faraday Soc.* **66**, 877 (1970).

- ⁶⁴See, for example, T. L. Hill, *Introduction to Statistical Thermodynamics* (Addison–Wesley, London, 1960).
- ⁶⁵G. Herzberg, *Infrared and Raman Spectra of Polyatomic Molecules* (Van Nostrand Reinhold, New York, 1945), p. 521 ff.
- ⁶⁶*Manual of symbols and Terminology for Physico-chemical Quantities and Units* (prepared by M. L. McGlashan, revision prepared by M. A. Paul, second revision by D. H. Whiffen) [Pure Appl. Chem. **51**, 1 (1979)].
- ⁶⁷Z. Slanina, Collect. Czech. Chem. Commun. **40**, 1997 (1975).
- ⁶⁸R. F. Hout, B. A. Levi, and W. J. Hehre, J. Comp. Chem. **3**, 234 (1982).
- ⁶⁹R. Zahradnik, Z. Slanina, and P. Carsky, Collect. Czech. Chem. Commun. **39**, 63 (1974).
- ⁷⁰Z. Slanina and R. Zahradnik, Collect. Czech. Chem. Commun. **39**, 729 (1974).
- ⁷¹H. L. Strauss and E. Thiele, J. Chem. Phys. **36**, 2824 (1967); F. M. Wachi and D. E. Gilmartin, High Temp. Sci. **4**, 423 (1972).
- ⁷²E. D. Simandiras, J. E. Rice, T. J. Lee, R. D. Amos, and N. C. Handy, J. Chem. Phys. **88**, 3187 (1988), and references therein.
- ⁷³D. A. Clabo Jr., W. D. Allen, R. B. Remington, Y. Yamaguchi, and H. F. Schaefer III, Chem. Phys. **123**, 187 (1988) and references therein.
- ⁷⁴J. M. L. Martin, J. P. François, and R. Gijbels, J. Comp. Chem. **10**, 152 (1989); *ibid.* (in press).
- ⁷⁵S. Becker and H. J. Dietze, Int. J. Mass Spectr. Ion Proc. **73**, 157 (1986).
- ⁷⁶H. J. Dietze and S. Becker, Fresenius Z. Anal. Chem. **321**, 490 (1985).